New Methods to Efficiently Test the Reliability of Plated Vias and to Model Plated Via Life from Laminate Material Data

Michael Freda
Sun Microsystems, Inc.

Dr. Donald Barker
Center for Advanced Life Cycle Engineering
University of Maryland

Abstract
This paper continues work by Sun Microsystems and the University of Maryland, CALCE[1] to predict plated through via life using laminate material properties, plated copper material properties, and the physical via geometry to model via life. The new method presented in this paper uses non-linear laminate material properties and a damage-fatigue model to predict the accumulated damage to a plated through via as it is thermally cycled through assembly and field life conditions.

Copper is a ductile metal so it is possible to construct a Log-Stress versus Log-Life plot that follows an Inverse Power Law (IPL).[2] The key to doing a Log-Stress versus Log-Life plot is developing the relationship of stress versus temperature of the laminate material. Use of a Log-Stress versus Log-Life plot allows increased testing efficiency since you can perform an accurate life analysis by testing at only the high and low temperature extremes. Once the Log-S versus Log-N plot is constructed, it is possible to predict plated through via life over a wide range of temperatures. For this paper, we will use thermal cycle to failure test data obtained from Interconnect Stress Test (IST),[3] but the analytical methods developed apply equally to other thermal cycle methods like Highly Accelerated Thermal Shock (HATS)[4] and Air-to-Air Thermal Shock (AATS).

Last, a Finite Element Model simulation is conducted that uses material properties that are easy to obtain and is then validated against the large database from IST testing at multiple temperatures. Once the Finite Element Model validation is complete, the model is used to make assembly and field life predictions for two case studies involving thick, complex printed wiring boards.

Keywords
Cycles to Failure, CTF, Finite Element Modeling, HATS, IST, Lead-Free, Miner's Rule, PTH Reliability, Via Reliability

Introduction
This paper is organized into the following sections:

1. Laminate Material Testing
2. Laminate Material Description
3. IST Testing
4. Summary of Cycle to Failure Analysis Estimates from Raw Data
5. Finite Element Model
6. Finite Element Analysis Results
7. Copper Fatigue Damage Law
8. Conclusion and Summary

1. Laminate Material Testing
An important first step in developing a stress versus temperature plot for a given laminate is obtaining laminate material data for CTE expansion versus temperature using TMA and modulus versus temperature using DMA. In previous work we used a combination of the raw TMA along with extrapolated CTE data for above and below T_g to predict expansion versus temperature from 25°C to 275°C. The extrapolated CTE values above and below T_g outside the test temperature range were calculated using algorithms in the TMA software.

The TMA testing protocol used on Laminate A consisted of three cycles from 25°C to 200°C using a ramp rate of 10°C per minute as called-out in IPC-TM-650 2.4.24c. Data from the third TMA cycle was used for the CTE expansion versus temperature plots. The TMA testing protocol used for Laminate B included the same initial three cycles from 25°C to 200°C followed by six cycles with a fast ramp rate from 60°C to 260°C to simulate lead-free assembly thermal stress followed by a 90 minute isotherm at 260°C for T_{260} testing. Appendix A includes a plot of the full TMA testing protocol used for both laminates.

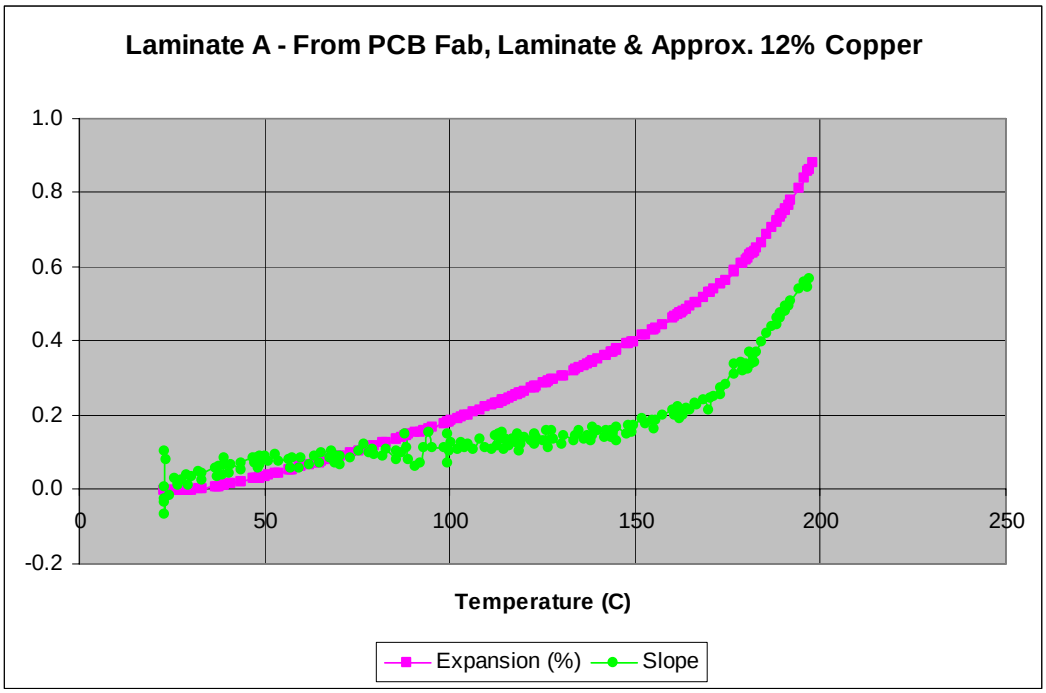

Figure 1.1 – Plot of expansion and slope for the 3rd TMA cycle of Laminate A.

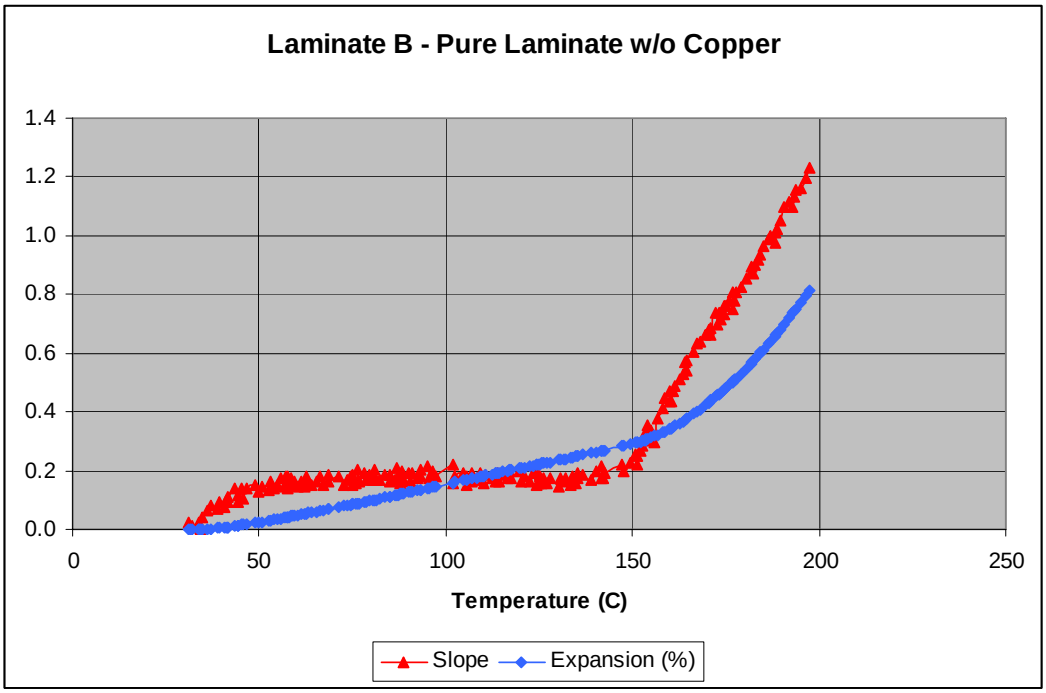

Figure 1.2 – Plot of expansion and slope for the 3rd TMA cycle of Laminate B.

One of the goals of our work is to develop via reliability predictions for different designs and different laminates. As a part of doing this, we began to look closely at the raw T_g data, see Figures 1.1 and 1.2. If you look at the slope for each laminate, you see the slope starts out relatively flat or linear and then increases with the onset of the transition from a glassy state to plastic phase at T_g. After that, the slope continues to increase and never flattens out past the T_g transition. Therefore, the test data from both Laminate A and B shows that the TMA testing did not continue to a high enough temperature and is still within the broad phase transition range at the 200°C peak TMA testing temperature. While this issue may be unique to

thermally resistant materials like those used in this study, in the future we will extend the peak TMA temperature to make sure it is sufficiently past the phase transition range.

One of the issues discussed during laminate testing is whether we should test samples constructed of only laminate material or use samples cut from actual pcb fabs that include copper layers and plated through holes (PTHs). While you can make an argument for either case, we decided to do the following:

- For Z-axis TMA expansion rate testing the preferred sample is from the actual pcb fab since the expansion rate and therefore the strain applied to the via is a function of the actual cross section of the pcb fab. Since more copper in the stack-up will lower the effective CTE because the CTE of copper is lower than the Z-axis CTE of laminate materials, we prefer the use a representative cross section that includes copper and is from the pcb fab being tested.
- For Z-axis TMA expansion rate testing we can use data obtained from pure laminate samples. Since the expansion rate of copper is well understood, we can take laminate data and adjust it for the copper percent of a particular stack-up and then calculate an expansion rate for the pcb fab with sufficient accuracy.
- For DMA modulus testing the samples must be pure laminate without copper. Since copper has a high modulus versus laminate materials, it is important to test only laminate material. For the best results, the sample should be representative of the glass styles and resin percent that will be used in the pcb fab.

A previously developed method[1] using TMA expansion versus temperature and modulus versus temperature was used to obtain Figure C.1 and Table C.2 in Appendix C which shows the relationship of temperature to stress for Laminate A.

2. Laminate Material Description

Laminate A is a non-dicyandiamide (aka non-dicy) cured epoxy/glass with filler added to lower the Z-axis CTE. Sun has successfully used this laminate for a number of years in products that are up to 3.5mm thick using eutectic tin/lead processing conditions. Laminate A has also performed well in lead-free testing of pcb fabs up to 4mm thick. Laminate B is a non-epoxy resin/glass system that Sun is testing for high aspect ratio, lead-free pcb fabs over 4mm thick. The mechanical properties for these two laminates are in Table 2.1. Of special note is the low expansion percent at 245°C for both laminate materials. Most epoxy/glass laminates have an expansion percent of 2.5% to 3.5% at 245°C. Also, the modulus of Laminate B is significantly lower than Laminate A. This results in lower stress since incremental stress is product of modulus times strain (i.e., strain due to the CTE expansion). Mechanical properties follow in Table 2.1.

Table 2.1 – Laminate material mechanical properties.

Property	Laminate A	Laminate B	Units
Z-axis CTE < T_g	45	50	ppm/°C
Z-axis CTE > T_g	200	180	ppm/°C
T_g by DSC	180	190	°C
T_g by TMA (estimate based on assumption TMA 10°C less than DSC T_g)	170	180	°C
Calculated Expansion at 245°C	2.03	1.85	%
Storage Modulus < T_g	18,000-15,000	7,350-6,600	MPa
Storage Modulus > T_g	2,500	1,500	MPa
T_g by DMA	162	170	°C

3. IST Testing

In our previous paper[1] we developed new methods to analyze thermal stress cycle to failure data of the type obtained from IST testing. In this section we would like to quickly use those techniques to analyze the expanded database that is now available.

The most commonly used IST test protocol has utilized preconditioning at assembly temperatures above the laminate T_g followed by cycle to failure below the laminate T_g. Plotting cycle to failure data versus stress allows us to take measurements in the T_g transition zone since we know the stress at these temperatures. Additional IST testing data was obtained in the T_g transition zone at 180°C and close to the T_g transition zone at 215°C. At both temperatures the IST coupons were cycled to failure at the test temperature indicated. We also performed additional testing at 150°C with this testing including preconditioning at 245°C. Tables 3.1 and 3.2 show the sample size obtained for each test condition.

Table 3.1 – IST sample size from testing ≥ the laminate material T_g.

Temperature	Previous Sample Size[1]	Current Sample Size
275°C	12	12
255°C	12	12
235°C	12	12
215°C	12	24 (+12)
180°C	0	24 (+24)
Total ≥ T_g	48	84 (+36)

Table 3.2 – IST sample size from testing with assembly preconditioning followed by CTF below T_g.

Preconditioning	Low Temperature	Previous Sample Size[1]	Current Sample Size
2x at 245°C	150°C	18	24 (+6)
6x at 245°C	135°C	12	12
6x at 245°C	150°C	18	18
10x at 245°C	120°C	6	6
10x at 245°C	135°C	12	12
10x at 245°C	150°C	18	24 (+6)
18x at 245°C	120°C	18	18
18x at 245°C	135°C	18	18
18x at 245°C	150°C	18	18
Total		138	150 (+12)

We are once again working with ductile metals which are known to follow an Inverse Power Law (IPL) relationship[1, 2] which we will use for our data analysis.

$$L(V) = \frac{1}{KV^n} \qquad \text{(Eq. 3.3)}$$

Equation 3.3 rearranges to a simple slope/intercept format after a Log-Log transformation to…

$$Ln[L(V)] = (-nLn \times V) + (Ln \times K) \qquad \text{(Eq. 3.4)}$$

Where: ***L*** represents the mean life of a plated via, i.e., $N_{50\%}$
V represents the stress level on the via in MPa
K is one of the model parameters to be determined, (K>0)
n is another model parameter to be determined

The data from IST testing at 180, 215, 235, 255, and 275°C was used for analysis with ReliaSoft's ALTA version 6.0 software to obtain an IPL/Lognormal best fit to the data. We used the cycles to failure data versus the stress at each test temperature (see Appendix C). A Lognormal distribution has been used over many years of via reliability testing at Sun. Lognormal has proved to be a better fit to cycle to failure data than other distributions like Normal, Exponential, or Weibull. Appendix D, Figure D.1 shows the poor fit to a Normal/Gaussian distribution while Figure D.2 shows the good fit to a Lognormal distribution.

Using equation 3.4 and solving for (aka fitting) coefficients ***K*** and ***n*** using ALTA (see the bottom left corner of the ALTA plots) we get the following:

$$L(V) = \frac{1}{K \times V^n} = \frac{1}{(9.7066 \times 10^{-21}) \times (V^{9.1684})} \qquad \text{(Eq. 3.5)}$$

Figures 3.6, 3.7, and Appendix E use this equation to estimate the $N_{50\%}$ cycles to failure at the various temperatures of interest in this study. In each plot the dark RED line on the right is the predicted cycles to failure at the chosen stress temperature using the data at 275, 255, 235, 215, and 180°C on the left.

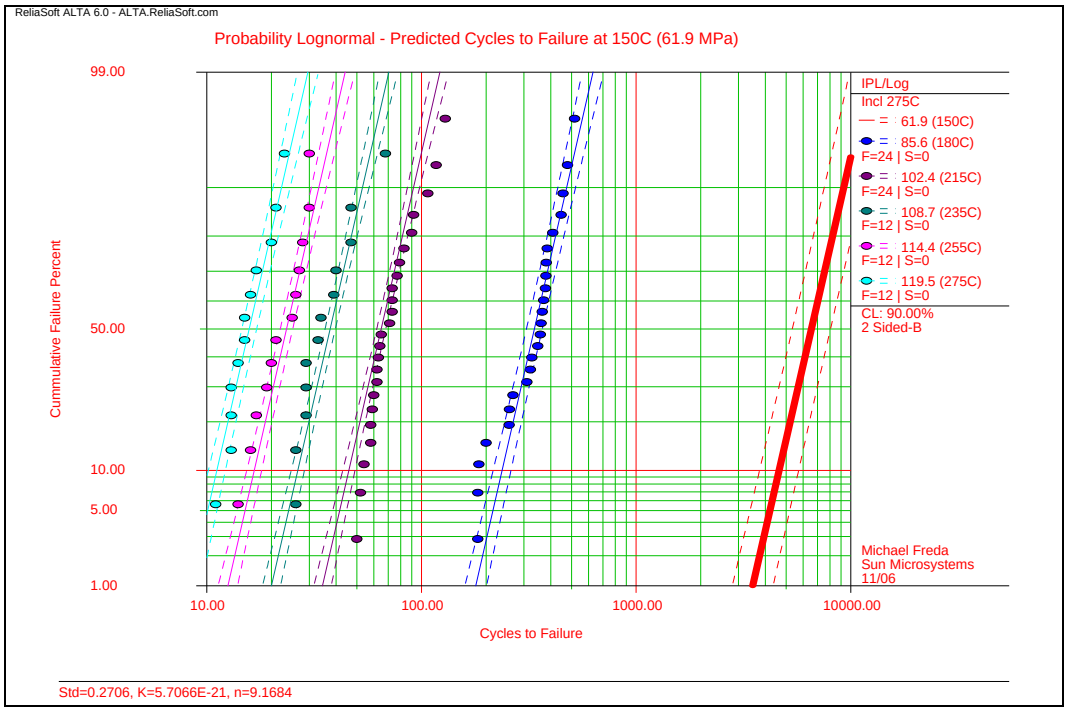

Figure 3.6 – IPL/Lognormal best fit to 180°C to 275°C data used to predict CTF at 150°C.

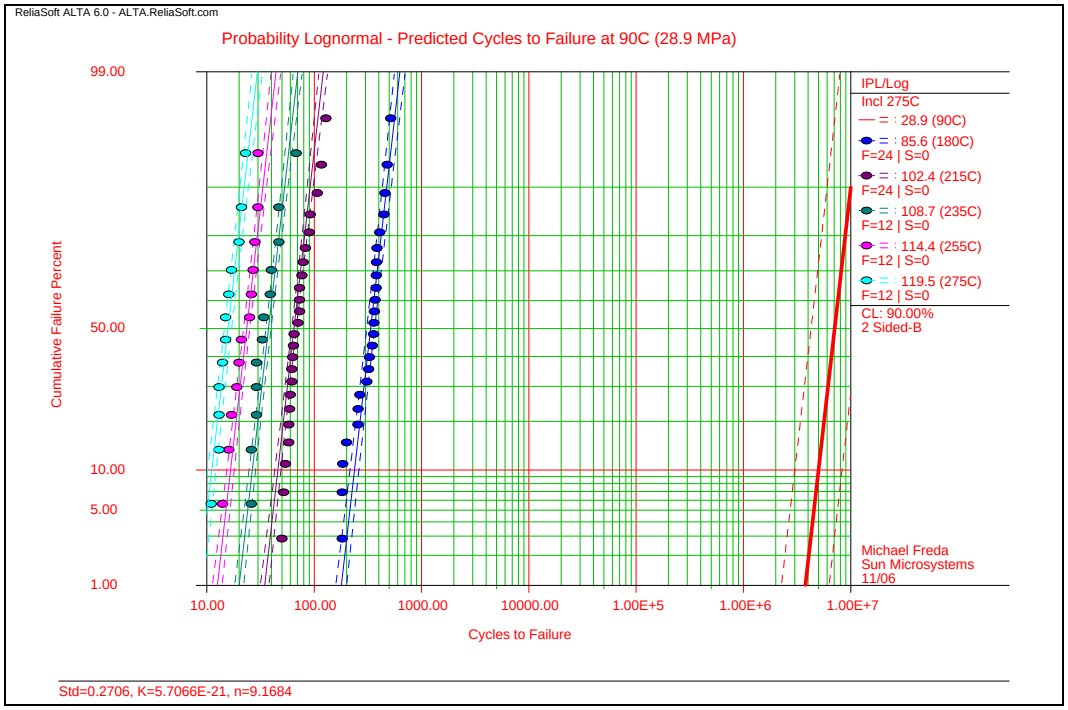

Figure 3.7 – IPL/Lognormal best fit to 180°C to 275°C data used to predict CTF at 90°C.

Figure 3.8 shows a composite plot of two of the analysis methods used in the paper. The RED scatter plot points show all the raw IST cycle to failure data where assembly precondition at 245°C was varied followed by IST cycling to failure at the temperature listed at the top of each plot. The RED dashed line shows the regression best fit to the Ln-S (assembly thermal stress) versus Log-N (cycles to failure), i.e., a classic Ln-S versus Ln-N plot. The data points circled are all outliers that were not used in the regression analysis. All of the outliers were from 18x preconditioning (i.e., 19x total thermal stress cycles including HASL). A careful review of Graph 4 in reference paper[1] shows that with 18x preconditioning we would expect about 2-14% of the IST coupons to fail or be close to failure after preconditioning. This is consistent with what we

experienced. In other words, our selection of 18x preconditioning was excessive, it would have been better if we had used a lower number like 15x.

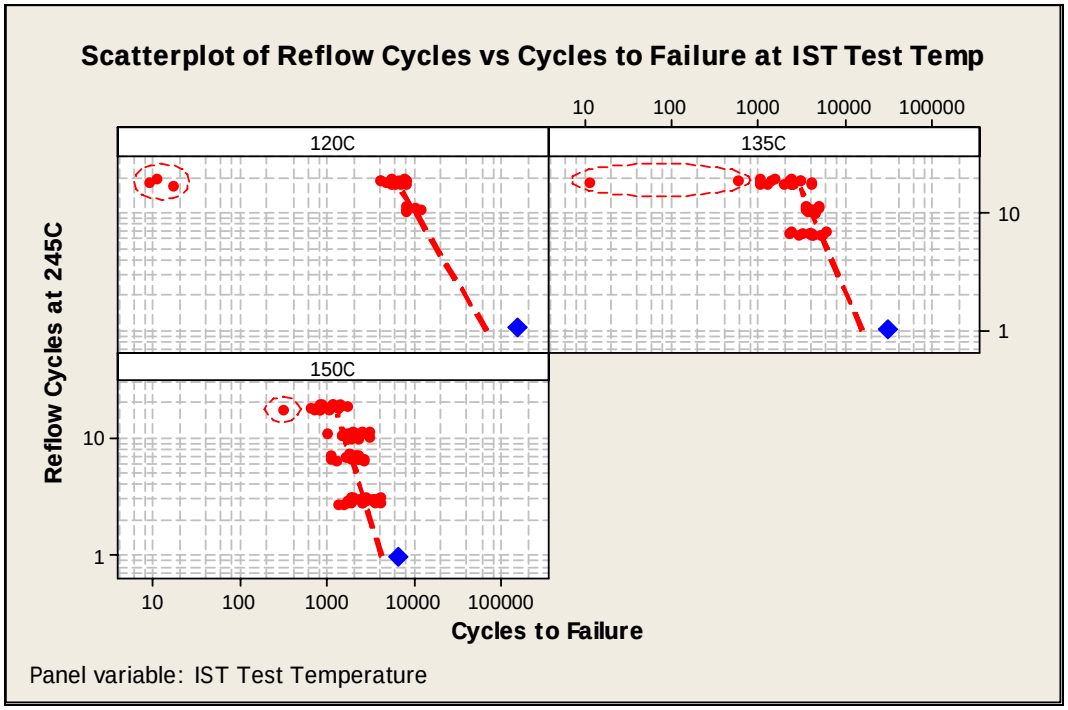

Figure 3.8 – Shows the Ln[assembly stress] versus Ln[CTF raw data] plots at 120, 135, and 150°C (i.e., data below T_g); the BLUE diamonds are the CTF estimates using an IPL/Lognormal Best Fit to 180°C to 275°C data (i.e., data above T_g); RED lines are the regression best fit, RED ellipses indicate outliners that were not used in the regression analysis.

The cycles to failure data obtained from testing at or above T_g at 180, 215, 235, 255, and 275°C and the IPL/Lognormal estimates using equation 3.5 are shown as a BLUE diamond. This method has a slightly higher cycles to failure estimate versus the regression method, but the two methods are in fairly good agreement.

4. Summary of Cycle to Failure Analysis Estimates from Raw Data

Finally, we quickly reran the Miner's Rule multiple regression method developed in our earlier work.[1] The analysis is in Appendix F and the results are in Table 4.1. This method gives the highest cycles to failure estimates of the three methods used. It is interesting that using the multiple regression method to solve for the Miner's Rule coefficients has twice resulted in a coefficient, C, that is noticeably less than 1. In our earlier work[1] C=0.68 and in the latest work C=0.34. The main difference between the two analysis runs is that 18x preconditioning data was not included in our second analysis and there was additional data at 150°C. It is possible that the reason that Miner's Rule coefficient C«1 is that the data in the analysis covers three fatigue regimes: the ultra-low cycle fatigue regime (<100 CTF), the low cycle fatigue regime (100 to 10,000 CTF), and the high cycle fatigue regime (>10,000 CTF).

Table 4.1 – Comparison of "As Received" cycles to failure estimates using the various analysis methods.

Temperature	Estimate from Figure 3.8	Reliasoft Alta IPL/Lognormal Analysis Using Equation 3.5	Miner's Rule, Appendix F	Range
150°C	4,100	6,600	16,000	3.9:1
135°C	17,000	31,000	66,000	3.9:1
120°C	64,000	150,000	200,000	3.0:1
90°C	---	7,100,000	---	---

Comparison of the cycle to failure estimates from the three analysis methods results in fairly good agreement with all the estimates within a range of 4x, well under one order of magnitude. Considering that one method used only data from testing above the T_g, but the estimated cycles to failure with this method falls in-between the estimates from the other two methods

using thermal cycling both above T_g (assembly preconditioning) and below T_g (IST cycling) combined with a fairly narrow range of estimates is encouraging.

5. Finite Element Model

Previously in the paper we showed how the raw data can be used with some relatively simple approaches to estimate the life of the PTH. In this section of the paper we use a non-linear finite element simulations with temperature dependent properties of the laminate to calculate the stress and strain within the PTH copper barrel. We used the general purpose finite element analysis (FEA) software ANSYS[13] for all our simulations. Since copper is a ductile material, the fatigue life is a direct function of the strain it experiences. The finite element model will then allow us to compare various thermal cycles and combinations of thermal cycles, both above and below and through the laminate glass transition region. The finite element model will also allow us to directly compare laminates with different mechanical properties.

Axi-symmetric finite element models of PTHs were built corresponding to the IST test coupons as well as future thicker specimens. Previous work in analyzing PTH life with finite element methods demonstrated that one did not need to model the full orthotropic properties of the laminate material and that an axi-symmetric model resulted in sufficient accuracy.[14] The axi-symmetric model can be visualized as a cross-section of the PTH spun around the centerline of the PTH hole. The axi-symmetric model is a pseudo 3-D model using only the out of plane Z-axis and radial r–axis dimension. All displacements in the circumferential or θ direction are zero. There were two basic PTH geometries. One for 3 mm thick laminates and another for 6 mm laminates. Table 5.1 summarizes the PTH dimensions.

Table 5.1 - PTH Geometry.

Laminate Thickness (mm)	PTH Drill Diameter (µm)	Copper Barrel Plating Thickness (µm)
3	350	30
6	400	30

The finite element mesh used 5, 8-noded quadrilateral elements through the thickness of the copper and laminate. Care was exercised to insure sufficient elements in both the Z-axis and radius-axis direction to keep the element aspect ratio less than 8. Mesh refinement exercises confirmed that the mesh was of sufficient density to accurately capture the response in the copper barrel. The axi-symmetric model can be thought of as a PTH in a circular section (actually a cylinder) of a laminate pc board. This cylinder of laminate material was on the order of 6 PTH drill-hole diameters in size. The outer wall of the cylinder of laminate material was constrained to move as a plane by tying the outer nodes to move in the radial direction together. The PTH was modeled as if it were a single PTH in an infinite laminate board. Previous work indicated that when PTHs are in an array structure, the nearest neighbors slightly reduce the stress and strain in the PTH by working together with neighbors to prevent the laminate from expanding in the z-direction.[14] We modeled the worst case, a PTH without nearby neighbors.

The copper in the FEM was modeled as a temperature independent ductile elastic-plastic material following a Ramberg-Osgood constitutive equation:

$$\varepsilon = \frac{\sigma}{E} + \left(\frac{\sigma}{K}\right)^{1/n} \qquad \text{(Eq. 5.2)}$$

where □ = von Mises stress, □ = effective strain (von Mises strain) and the elastic modulus E=120 GPa, Ramberg-Osgood parameters K=0.631 GPa, n=0.15[14]. Copper CTE was a constant 17 ppm/°C and Poisson's ratio = 0.35. The various laminates were modeled as elastic materials with a temperature dependent CTE and temperature dependent elastic modulus, E. The finite element model treated the laminate as a homogenous material and ignored the laminate inner plane copper layers. This is a reasonable approach since the temperature dependent properties measured in the TMA and DMA tests were effective properties of the actual laminate structure containing the copper trace layers. Figure 5.3 and Figure 5.4 show schematically the laminate temperature dependent properties that were entered into a lookup table within the ANSYS model and is a representation of the property values used at each temperature step in the analysis.

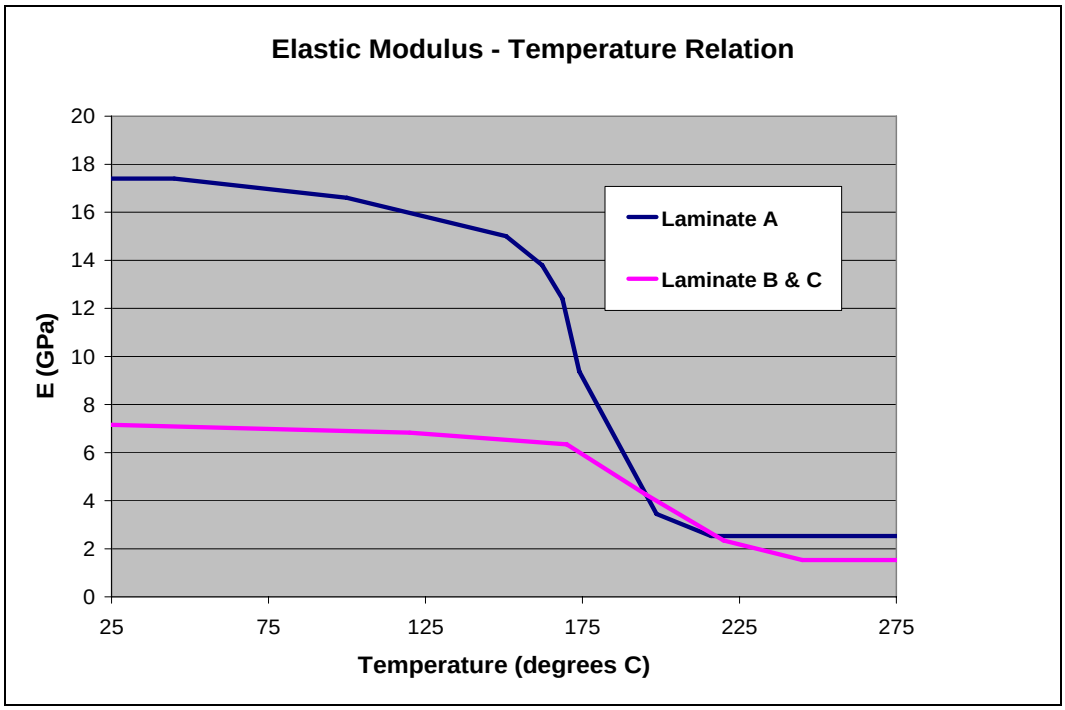

Figure 5.3 - Temperature dependent laminate elastic modulus, E, used in the finite element modeling.

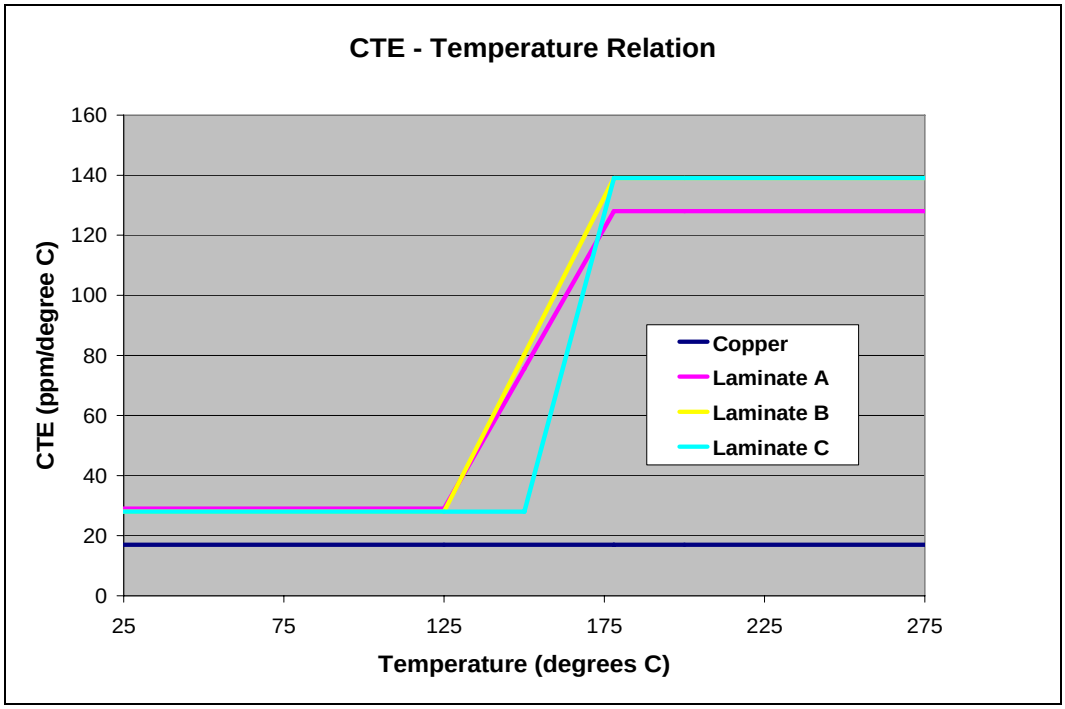

Figure 5.4 - Temperature dependent laminate CTE used in the finite element modeling.

The PTH finite element model was subjected to a simulated IST thermal cycle that ranged from a low temperature of 25°C to various high temperatures, and back in a cyclic fashion. The complete thermal cycle going from low to high to low again took 10 minutes. At these temperature ranges, copper experiences negligible creep and acts like a time independent ductile material. Due to lack of creep properties for the laminate materials, the laminates were also assumed to experience negligible creep. For these reasons, and since the model assumed thermal equilibrium at every incremental temperature step, the period of the temperature is actually irrelevant.

The PTH barrel copper and board laminate were assumed to be initially stress free at room temperature. The PTH FEA model was then subjected to multiple thermal cycles and the stress and strain in the PTH barrel monitored. Past experience, as well as confirmed with analyses here, indicates that shake down and ratcheting stabilizes by the third thermal cycle. On the third thermal cycle the stress and strain response is representative of any later cycle and independent of the initial stress free temperature. By the third thermal cycle the stress and strain value at the beginning and end of every cycle are nearly the same value and a plot of stress versus strain follows the same loci. Figure 5.5 is a representative plot of the copper stress versus plastic strain on the third thermal cycle going from 25°C to 245°C. The area within this plot or hysteresis loop is a measure of the copper plastic strain energy density, or one measure of the damage done by the thermal cycle. The critical fatigue damage parameter that we are using in this paper is the plastic strain range as indicated in the figure.

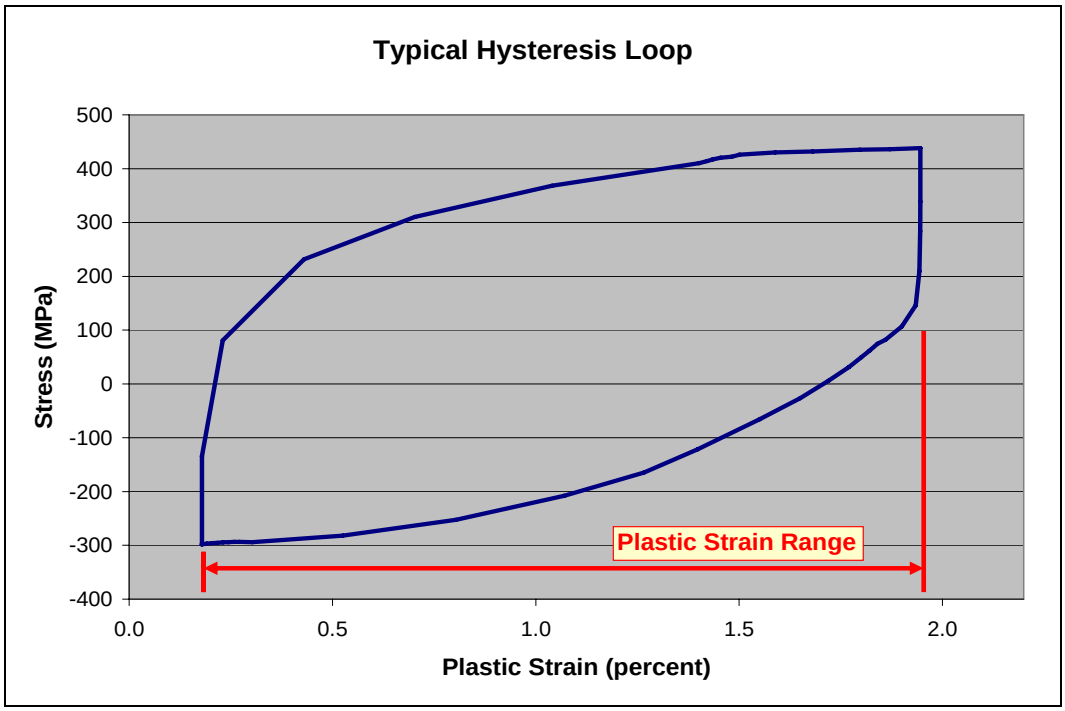

Figure 5.5 - Typical hysteresis loop for the 3rd thermal cycle showing the plastic strain range in the PTH copper barrel.

The FEA model clearly showed that the maximum strain range in the copper barrel was in the mid-plane region of the laminate board. This directly correlates with the observed location of barrel cracks seen in cross sections of failed samples. Subsequent analyses results used the stress and strain range of a copper barrel element located on the exact mid-plane of the laminate board and in the middle of the copper plating thickness.

6. Finite Element Analysis Results

Table 6.1 is a summary of the copper barrel maximum strain ranges for Laminate A under various temperature cycles. In the table the thermal cycle is designated by only the maximum temperature.

Table 6.1 - Copper barrel maximum strain range during a thermal cycle, 3mm thick, Laminate A.

Maximum Temperature	Plastic Strain Range (%)	Total Strain Range (%)
275°C	2.554	2.739
255°C	2.296	2.505
245°C	2.193	2.399
235°C	2.091	2.304
215°C	1.916	2.114
200°C	1.819	2.025
170°C	1.342	1.540
150°C	0.401	0.604
135°C	0.043	0.221
120°C	0.000	0.101

7. Copper Fatigue Damage Law

Previously in the paper we reintroduced the Inverse Power Law (IPL):[2]

$$L(V) = \frac{1}{KV^n} \qquad \text{(Eq. 7.1)}$$

for calculating the life, L, of PTHs as a function of a damage parameter, V, with fitting parameters K and n. In the classical metal fatigue literature, this IPL relation is well known as the Manson-Coffin fatigue equation where the fatigue damage parameter is the plastic strain range $\Delta\varepsilon_{plastic}$. Using the more common notation of the metal fatigue community the Manson-Coffin equation is written as:

$$\frac{\Delta\varepsilon_{plastic}}{2} = \varepsilon_f (2N_f)^c \qquad \text{(Eq. 7.2)}$$

or solving directly for cycles to failure, N_f, the equation is more recognizable as the IPL, equation 3.3 and 7.1:

$$N_f = \frac{1}{2}\left[\frac{\Delta\varepsilon_{plastic}}{2\varepsilon_f}\right]^{1/c} \qquad \text{(Eq. 7.3)}$$

In the metal fatigue community c is known as the fatigue exponent and ε_f is known as the fatigue constant. Both are really just fitting parameters. Regardless of the form of the equation used, the important point is that low cycle fatigue life is directly a function of the plastic strain range. The FEA model allows us to calculate the copper plastic strain range. Thus it is possible to directly calculate the fatigue life of the PTH if one knows the fatigue constant and fatigue exponent (fitting parameters for the IPL).

In the IST thermal cycling experiments, the copper barrel fatigue cracks occur in different fatigue regimes. The IPL is still applicable in each fatigue regime, but the fitting constants are a function of the fatigue regime. The IST thermal cycle above the glass transition temperature causes such large plastic strains in the copper barrel that the PTHs fail in less than 100 cycles. Failures occurring in such a small number of cycles are considered to be in the ultra-low cycle fatigue regime. Failures occurring between about 100 cycles and about 10,000 are in the classical area known as low cycle fatigue. In the low cycle fatigue regime, the damage per cycle is not as severe as in the ultra low cycle fatigue regime. For failures between about 10,000 to 100,000 cycles, the fatigue regime is a transition region between classic low cycle fatigue and high cycle fatigue. In this regime the total strain, elastic strain plus plastic strain, drives the fatigue damage. For failures above about 100,000 cycles, one is in the high cycle fatigue regime and damage is due to elastic strain. In the high cycle fatigue regime there is negligible plastic strain.

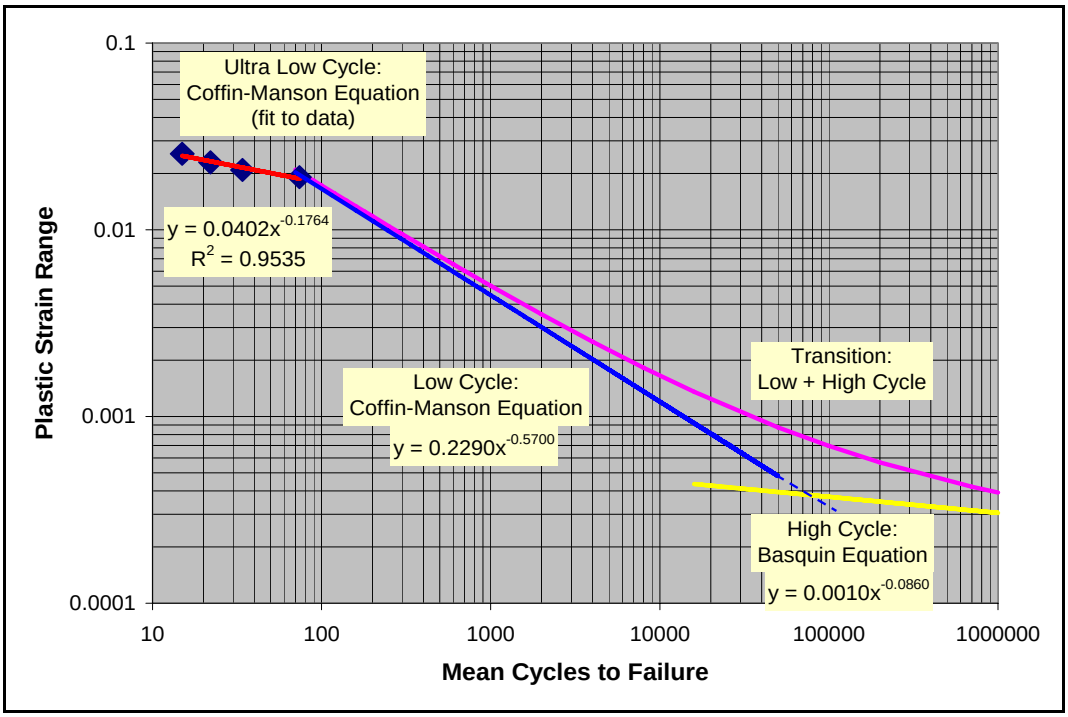

Figure 7.4 - PTH copper barrel fatigue relations in the ultra-low, low, and transition region between low and high cycle fatigue regimes.

The copper ultra low cycle fatigue exponent, *c*, and constant, $_f$, are not known, but can easily be determined from the FEA simulations and IST experimental results for the cycles conducted above the glass transition temperature. In Figure 7.4 the 4 data points are the plastic strain range calculated from the FEA simulations and the experimentally determined mean life, $N_{50,}$ for IST run to failure at 275, 255, 235, and 215°C. A least squares power law fit to the data is shown as the red line in the figure along with the resulting equation. The ultra low cycle copper fatigue exponent is thus *c=-0.18* or *n=-1/c=5.67* and the fatigue constant as indicated in the equation. The blue line in the figure represents a previously determined fatigue relation for PTH copper in the low cycle fatigue regime.[14] The fatigue exponent in this regime was *c=-0.57* and the fatigue constant $_f$ *=0.17*. The increase in the absolute value of the fatigue exponent, steeper slope in the log-log plot of cycles to failure versus plastic strain range going between ultra low cycle fatigue regime and the low cycle fatigue regime is expected since the damage per cycle is not as severe.

Failures in the region between about 10,000 cycles to about 100,000 cycles are in the transition region between low and high cycle fatigue where the damage is due to both elastic and plastic strain. In this transition region the fatigue damage law can be expressed as a combination of the Coffin-Manson equation, used in the low cycle fatigue regime, and the Basquin equation, used in the high cycle fatigue regime. The combined fatigue equation is commonly written as:

$$\frac{\Delta\varepsilon_{total}}{2} = \frac{\Delta\varepsilon_{elastic}}{2} + \frac{\Delta\varepsilon_{plastic}}{2} = \frac{2S_u}{E}\left(2N_f\right)^b + \varepsilon_f\left(2N_f\right)^c \qquad \text{(Eq. 7.4)}$$

where the total strain range can be broken into its elastic and plastic contributions. The new constants in the high cycle equation are *Su* – stress term related to the ultimate strength, *E* – Young's Modulus, and the high cycle fatigue exponent *b*.

The yellow line in Figure 7.4 is the high cycle fatigue relation, Basquin equation. The magenta line in the figure is the combined low and high cycle fatigue relation expressed in equation 7.4. Note in the figure that below about 10,000 cycles the contribution of the elastic strain is small and the solid blue line of the Coffin-Manson equation is adequate by itself as a damage law. Above, 10,000 one definitely needs to also consider the elastic strain in the damage law.

Using the fatigue damage equations as shown in Figure 7.4 one can determine the life of a PTH subjected to any thermal cycle from the copper strain calculated from the finite element simulation. The fatigue equations determine the life for a particular thermal cycle. If one subjects a PTH to a series of thermal cycles, such as preconditioning thermal cycles followed by lower temperature cycles, one can use a simple linear damage superposition technique to calculate when the PTH will fail. The simple linear damage superposition technique is commonly known as Miner's Rule and is expressed as:

$$\frac{n_1}{N_1}+\frac{n_2}{N_2}+\cdots+\frac{n_m}{N_m}=C \qquad \text{(Eq. 7.5)}$$

Where n_i is the number of cycles that the PTH experiences for the i^{th} thermal cycle, N_i is the number of cycles to failure if the PTH were only exposed to the i^{th} thermal cycle, and C is the total damage fraction constant and typically varies in value from about 0.5 to 1.5. For the case with preconditioning cycles followed by a lower temperature thermal cycle we can solving for the unknown number of cycles that the IST coupons will last after preconditioning:

$$n_2 = N_2\left(C-\frac{n_{precondition}}{N_{precondition}}\right) \qquad \text{(Eq. 7.6)}$$

Both N_2 and $N_{precondition}$ can be determined from the fatigue relations shown in Figure 7.4 and the calculated plastic strain range from the FEA simulations. Table 7.7 is the results of the above equation for Laminate A where the number of preconditioning cycles, $n_{precondition}$, is specified and the table lists the number of cycles the PTH will last at various lower temperature cycle peaks, where the constant C was assumed to be exactly 1.0. The results in Table 7.7 are also plotted in Figure 7.8 which is the previously discussed Figure 3.8 showing the regression fit to the raw IST data and the estimate using only IST data above T_g and the IPL/Lognormal method.

Table 7.7. - Calculated cycles to failure after various numbers f preconditioning cycles at 245 ºC for Laminate A.

	Precondition Cycles at 245°C + 1 HASL Cycle			
IST T_{max}	**3x**	**7x**	**11x**	**19x**
120 ºC	12249	10503	8757	5266
135 ºC	3106	2663	2220	1335
150 ºC	1091	936	780	469

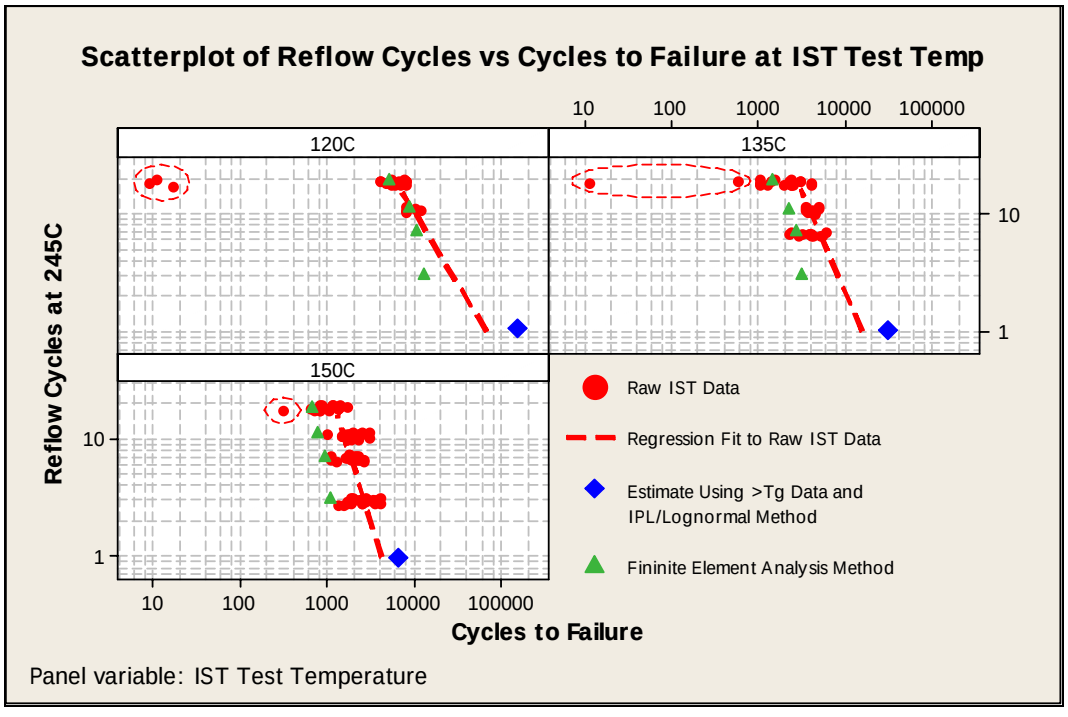

Figure 7.8 – Same plot as Figure 3.7 with the addition of FEA modeling results which are overlaid using the GREEN triangles.

The non-linear FEA results can be used to easily compare the response or life of a PTH in different laminates. Figure 5.3 and 5.4 previously showed the temperature dependent properties of three different laminates used in FEA simulations. Sun had experience with Laminate A and was interested in the relative performance of Laminate B (Laminate C properties were

identical to Laminate B except the beginning of the glass transition phase was slightly elevated). Table 7.8 is a summary of the various strain ranges for a 245ºC cycle. The ratio of the calculated plastic strain ranges for Laminate B over the plastic strain range for Laminate A when subjected to a 245ºC preconditioning cycle is $\Delta\varepsilon_{pB}/\Delta\varepsilon_{pA}=0.86$ for the 3mm laminates. Using the IPL the ratio of life, N_B/N_A, is simply:

$$\frac{N_B}{N_A}=\left(\frac{\Delta\varepsilon_B}{\Delta\varepsilon_A}\right)^{1/c}=(0.86)^{1/-.18}=2.3 \qquad \text{(Eq. 7.9)}$$

Laminate B will last 2.3 times longer under a 245ºC thermal cycle (3mm thick laminate).

Table 7.10 - Calculated strain ranges for a 245°C cycle for various laminates.

Laminate Thickness	Laminate	Plastic Strain Range $\Delta\varepsilon_p$ (%)	Total Strain Range $\Delta\varepsilon$ (%)	$\frac{\Delta\varepsilon_{pB}}{\Delta\varepsilon_{pA}}$
3mm	A	2.193	2.399	
	B	1.890	2.103	0.862
6mm	A	2.465	2.673	
	B	2.235	2.433	0.907

For a lower temperature thermal cycle shown in Table 7.9, maximum temperature 150ºC, the ratio of plastic strain ranges is 0.74 for the 3mm thick case. For this lower temperature cycle the fatigue exponent is $c=-0.57$. The life ratio is thus $N_B/N_A = 1.7$. A PTH in laminate B lasts 1.7 times longer than a PTH in laminate A. Laminate C, which does not enter the glass transition region compared to Laminate A, lasts much longer, $N_C/N_A \sim 20$ (for the N_C/N_A comparison, the total strain range must be used).

Table 7.11 - Calculated strain ranges for a 150°C cycle for various laminates.

Laminate Thickness	Laminate	Plastic Strain Range $\Delta\varepsilon_p$ (%)	Total Strain Range $\Delta\varepsilon$ (%)	$\frac{\Delta\varepsilon_{pB}}{\Delta\varepsilon_{pA}}$	$\frac{\Delta\varepsilon_C}{\Delta\varepsilon_A}$
3mm	A	0.401	0.602		
	B	0.295	0.510	0.737	
	C	0.000	0.098		0.163
6mm	A	0.463	0.668		
	B	0.349	0.551	0.753	
	C	0.000	0.116		0.173

The FEA simulation allows one to conduct a sensitivity study to determine the critical property of the laminate that most strongly influences the plastic strain and thus the life. Figure 5.3 shows that the elastic modulus of Laminate B starts out at less than half the value of Laminate A at lower temperatures, but in the upper temperatures Laminate B is only slightly lower than Laminate A. One could physically argue that the lower elastic modulus of Laminate B would result in a lower plastic strain in the PTH. This is born out in the simulation where the elastic modulus of Laminate A and B were used, but the temperature dependence on CTE was kept artificially the same as either Laminate A, B, or C (total of six combinations for each temperature cycle). For the preconditioning cycle of 245ºC the lower modulus of Laminate B resulted in an average decrease in plastic strain range of $\Delta\varepsilon_{pB}/\Delta\varepsilon_{pA}=0.75$, which corresponds to an increase in life of about 5 times. For the lower temperature cycle going to 150ºC, the lower modulus of Laminate B resulted in an average decrease in plastic strain range of about $\Delta\varepsilon_{pB}/\Delta\varepsilon_{pA}=0.64$, which corresponds to an increase in life of about 2 times.

Similarly, the influence of the CTE was determined by artificially keeping the elastic modulus response the same across cases (again 6 combinations for each temperature cycle). Figure 5.4 shows that the CTE of material A and B are nearly the same below T_g, but Laminate A has a lower CTE above the T_g region. The CTE of Laminate C is identical to Laminate B, except

that the beginning of the T_g region for laminate C is higher than Laminate B. Physically one could argue that above T_g material B and C would generate more plastic strain than Laminate A. The simulations showed that for the 245ºC preconditioning cycle Laminate B and C generated 1.16 times more plastic strain the Laminate A. This results in a reduction of life for Laminate B and C of about 0.44 times Laminate A. As discussed above, the elastic modulus alone for Laminate B and C resulted in about a 5 time increase in life. It is clear from these results that the elastic modulus has the most influence on life for the preconditioning cycle. For the 150ºC lower temperature cycle, Laminate B again generates about 1.16 more plastic strain than Laminate A. At these lower temperatures the reduction in life is only about 0.78 times for the CTE only and about a 2 time increase in the life for the elastic modulus only. Again the elastic modulus has the most influence on the life. For Laminate C, 150ºC is still below its T_g region and thus the strain generated is much smaller than for Laminate A which entered the T_g region at 125ºC. The elastic modulus dominates the response for Laminate C.

The influence due to the increase in laminate thickness from 3 mm to 6mm is easily seen from the FEA simulations. On average for the different laminates, the increased plastic strain in the 6mm laminate resulted in a decrease in life of a PTH as compared to the life in a 3mm laminate, $N_{6mm}/N_{3mm}=0.5$ for the 245 ºC cycle and $N_{6mm}/N_{3mm}=0.75$ for the 150 ºC cycle.

8. Conclusion and Summary

The work presented in the first half of this paper verifies an improved thermal analysis method of plated through via life that combines the laminate material mechanical properties of CTE expansion versus temperature and modulus versus temperature to develop a stress versus temperature relationship. That stress versus temperature relationship is then used to perform an IPL/Lognormal analysis of cycle to failure data versus stress to allow the estimation of plated via (PTH) life over a wide range of stresses and temperatures.

In the second half of this paper, a non-linear finite element model (FEM) is developed that uses the temperature dependent properties of the laminate material to calculate the stress and strain within the PTH copper barrel. This axi-symmetric, FEM uses the laminate properties from TMA and DMA testing. The calculated strain in the copper barrel is then used in conjunction with copper fatigue damage models to predict PTH cycles to failure. Comparison of the FEM results using Laminate A shows a good agreement to the PTH reliability database and to the IPL/Lognormal estimates from the first half of the paper. FEM simulation also allows one to quickly compare PTH life in various laminate materials as well as different board thicknesses and PTH geometries. These rapid comparisons help one to quickly identify the better design and/or material. Sensitivity studies can be easily conducted to determine the critical material property or PTH dimension. In this paper, it was shown that the primary advantage of Laminate B over Laminate A was due to the difference in the temperature dependent elastic moduli and not due to the difference in CTE.

References

1. Don Barker and Michael Freda, "Predicting Plated Through Hole Life at Assembly and in the Field from Thermal Stress Data," Proceedings of IPC/APEX 2006, Anaheim, CA, 8-10 February 2006.
2. J.E. Shigley and C.R. Mischke, Mechanical Engineering Design, Fifth Edition, McGraw-Hill Book Company, pages 309-311, 1989.
3. www.pwbcorp.com
4. www.hats-tester.com
5. Jingsong Xie, Yu-Jie Huo, Yuan Zhang, Michael Freda, "Effect of PWB Factors and Glass Transition Temperature on PTH Reliability," 39th International Symposium on Microelectronics, San Diego, California, October 11, 2006.
6. Jason Furlong, Michael Freda, "Application of Reliability/Survival Statistic to Analyze Interconnect Stress Test Data to Make Life Predictions on Complex, Lead-Free Printed Circuit Board Assemblies," Cologne, Germany, Proceedings of EPC 2004, 5 October 2004.
7. Michael Freda, "Interconnect Stress Testing, Historical Baseline Cycle to Failure Data and Analysis Results from Upcoming Generation of Lead-Free Servers," Dongguan, Peoples Republic of China, HKPCA 2004 Conference, 9 December 2004.
8. "Inverse Power Relationship Introduction," at www.weibull.com/AccelTestWeb/inverse_power_law
9. Don Barker, Craig Hillman, et al, Meeting at University of Maryland, College Park, MD., 12 May 2005.
10. Don Barker, private email on Storage and Loss Modulus, 25 July 2005.
11. Don Barker, Meeting at University of Maryland to discuss method to develop the stress on copper versus temperature curve, College Park, MD., 18 May 2005.
12. Joe Smetana, Ken Ogle, "Via (Plated Through Hole) Integrity with Lead-Free Soldering," Proceedings of IPC/APEX 2006, Anaheim, CA, 8-10 February 2006.
13. ANSYS Inc, Southpointe, 275 Technology Drive, Canonsburg, PA 15317 or http://www.ansys.com
14. Barker, Donald B. and Abhijit Dasgupta, "Thermal Stress Issues in Plated-Through-Hole Reliability", Thermal Stress and Strain in Microelectronics Packaging, edited by John Lau, Van Nostrand Reinhold, 1993.

15. Ashby, Michael F. and Jones, David R.H., "Chapter 15, Fatigue Failure," Engineering Materials 1, Second Edition, Butterworth-Heinemann, 1996.

Appendix A – Full Plot of TMA Testing Protocol

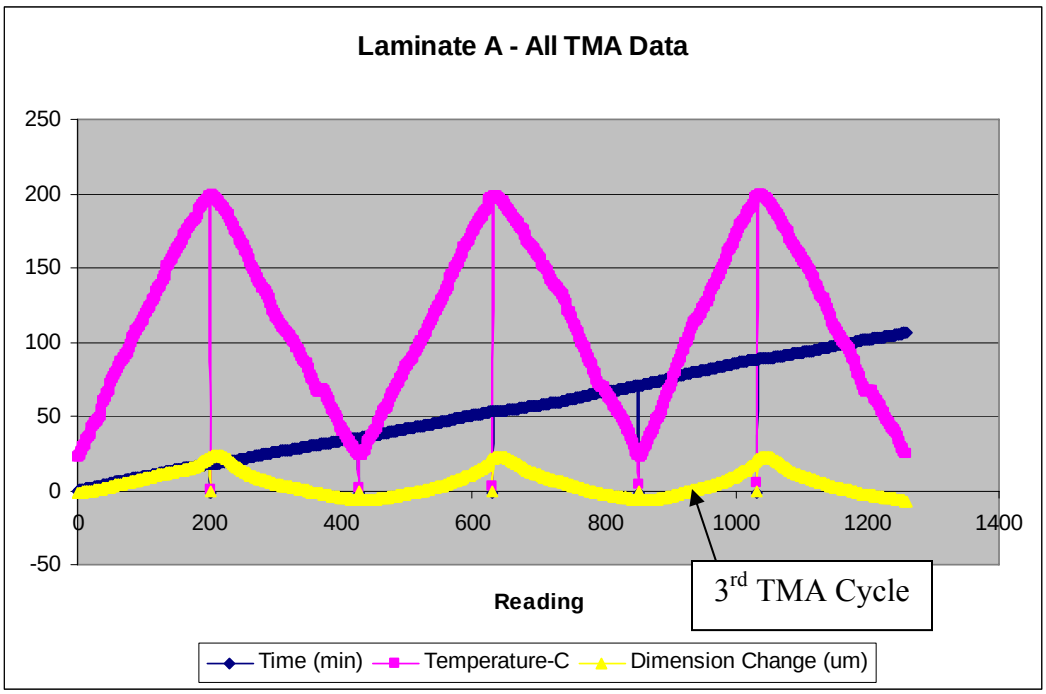

Figure A.1 – Laminate A using an older TMA testing protocol, expansion data was taken from the 3rd TMA cycle.

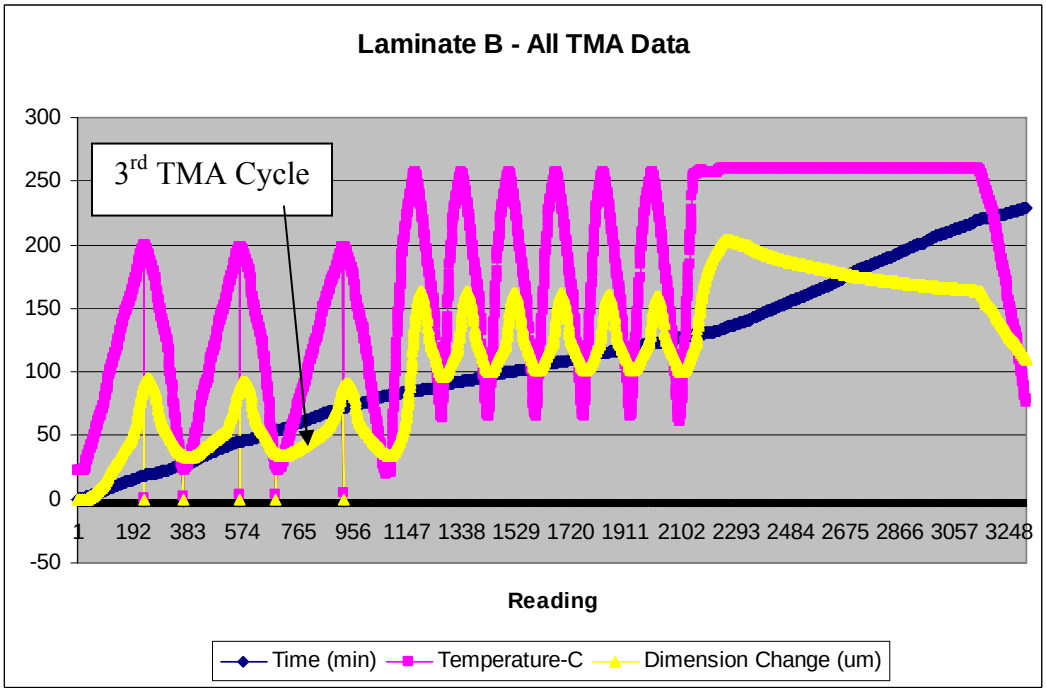

Figure A.2 – Laminate B using the latest TMA testing protocol, expansion data was taken from the 3rd TMA cycle.

Appendix B – Plot from DMA Testing

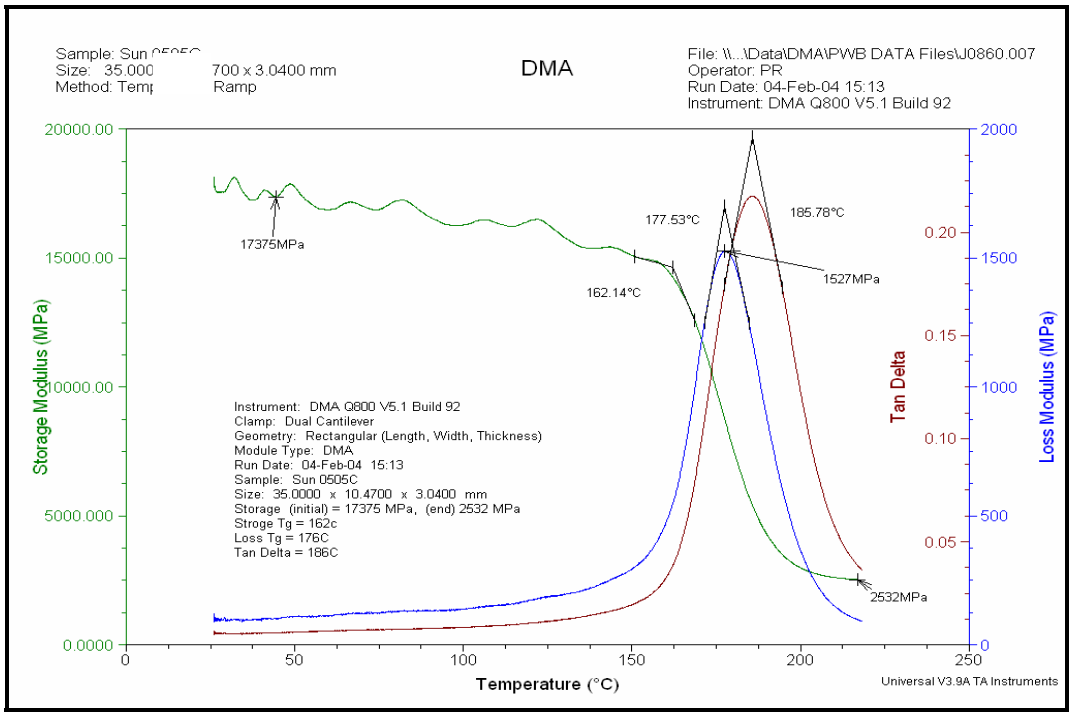

Figure B.1 – DMA of laminate A.

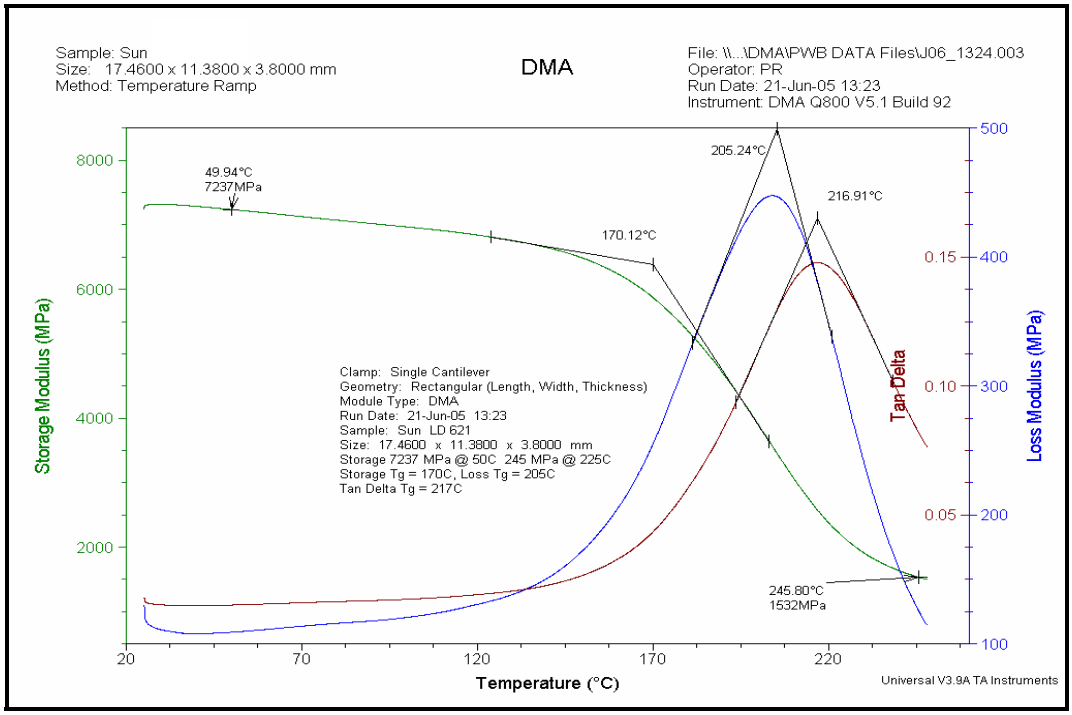

Figure B.2 – DMA of laminate B.

Appendix C – Cumulative Stress versus Temperature

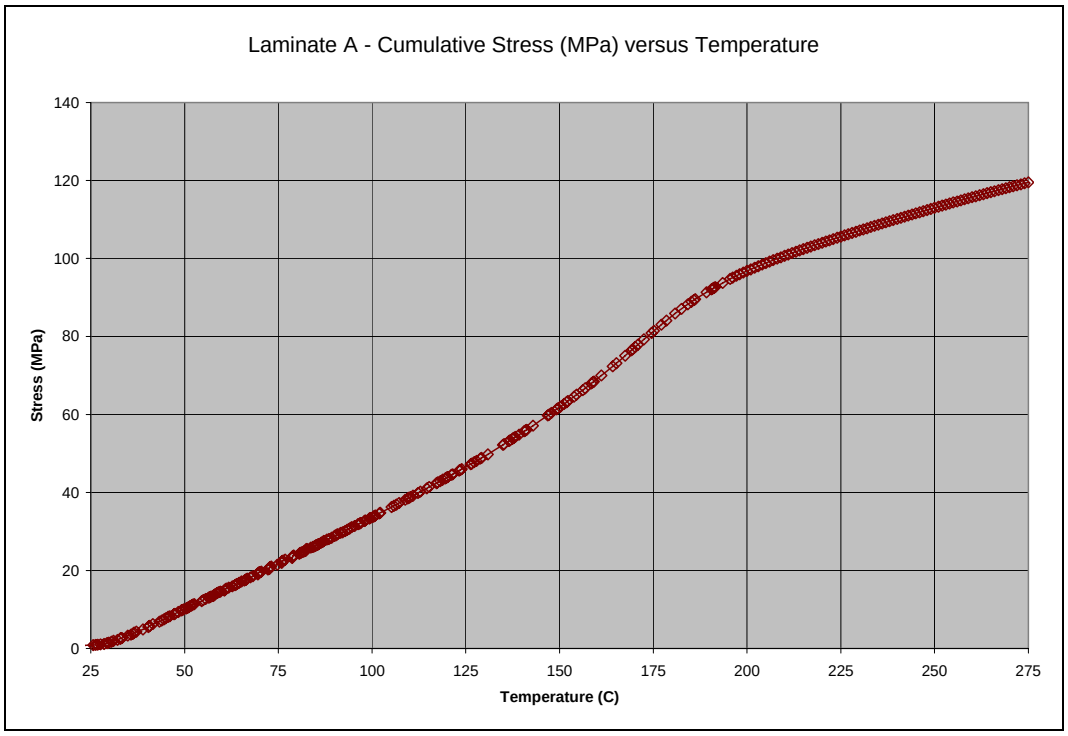

Figure C.1 – Stress versus temperature plot obtained from TMA expansion data and DMA modulus data.

Table C.2 – Stress at selected temperatures for laminate A.

Temperature	Stress (MPa)	Stress (PSI)
90°C	28.9	4,190
120°C	43.9	6,370
135°C	52.3	7,590
150°C	61.9	8,980
180°C	85.6	12,400
215°C	102.4	14,850
235°C	108.7	15,770
245°C	111.6	16,180
255°C	114.4	16,590
275°C	119.5	17,330

Appendix D – Normal histogram and Ln(Normal) histogram of CTF data at 150°C.

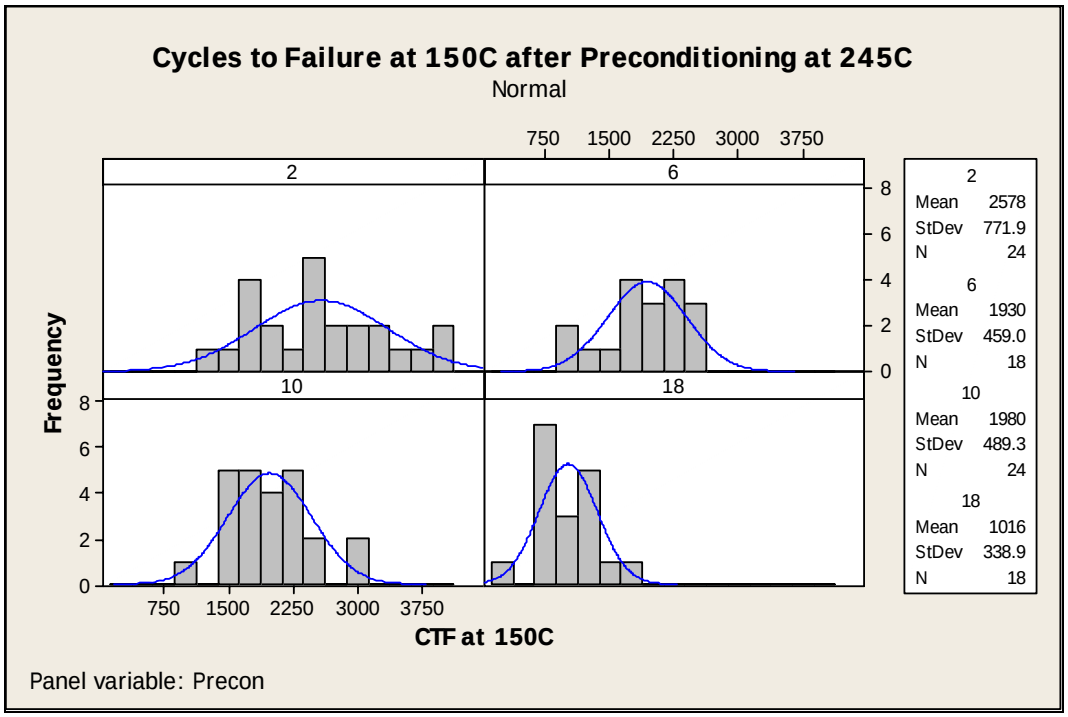

Figure D.1 – Histogram of IST cycle to failure data on pcb fabs constructed with laminate A. Note the data shows a <u>poor</u> fit to a Normal/Gaussian distribution.

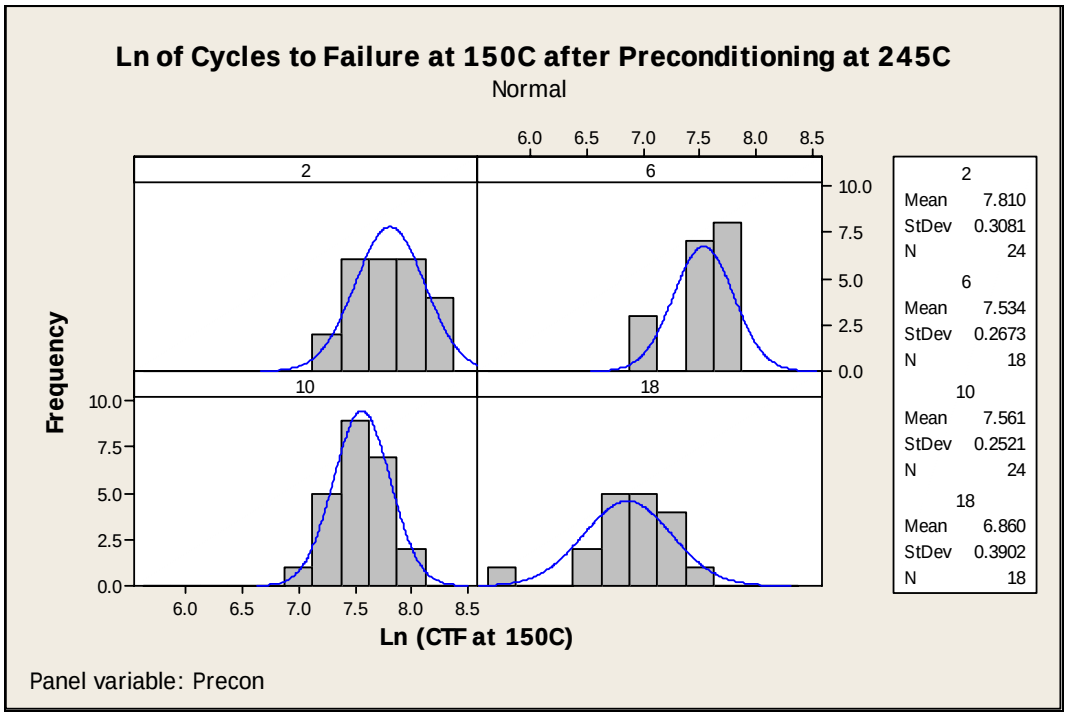

Figure D.2 – Histogram of IST cycle to failure data on pcb fabs constructed with laminate A. Note the data shows a <u>good</u> fit to a Lognormal distribution.

Appendix E – IPL/Lognormal Estimates of CTF at Lower Temperatures

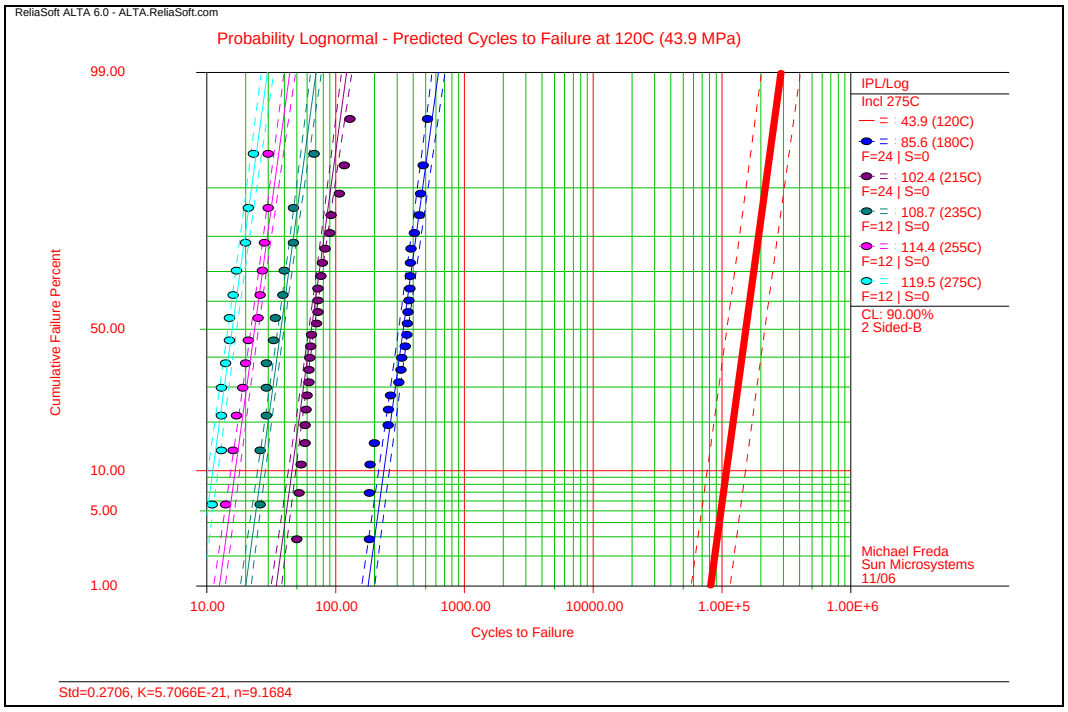

Figure E.1 – IPL/Lognormal best fit to 180°C to 275°C data used to predict CTF at 120°C.

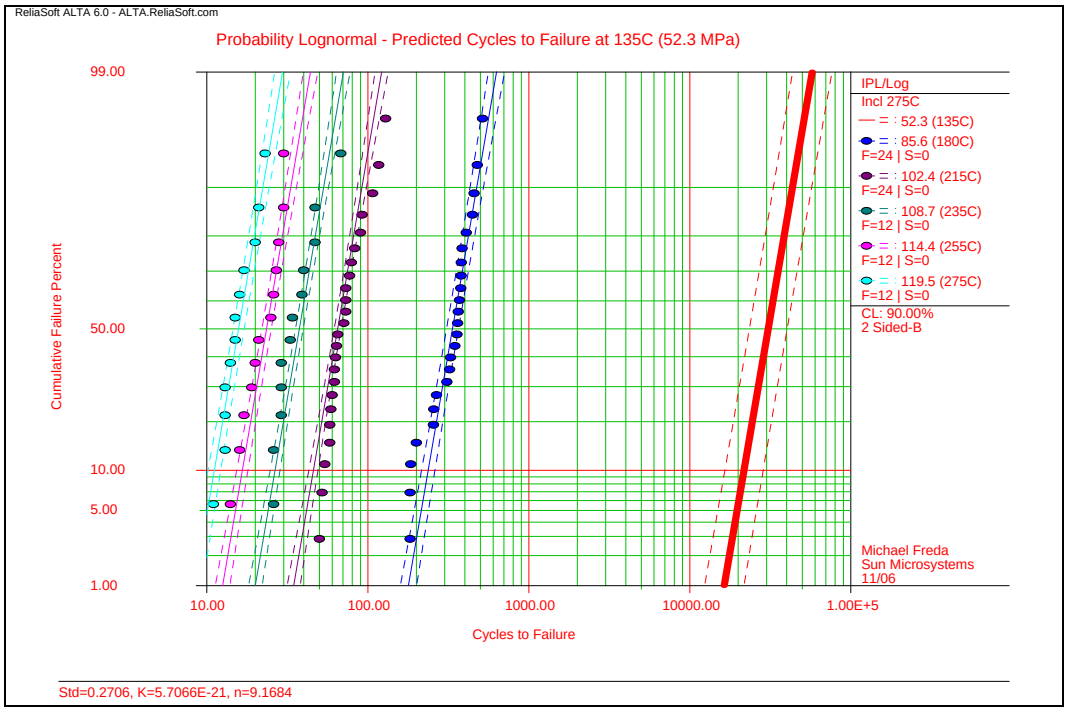

Figure E.2 – IPL/Lognormal best fit to 180°C to 275°C data used to predict CTF at 135°C.

Appendix F – Regression Analysis Using Miner's Rule

Regression Analysis: -(n245 x INV-N245) versus n120, n135, n150

The regression equation is:

$$-\left(n_{245} \times INV_{245}\right) = 0.3414 - \left(0.0000051 \times n_{120}\right) + \left(0.00001522 \times n_{135}\right) + \left(0.00006186 \times n_{150}\right) \quad \text{(Eq. F.1)}$$

Predictor	Coef	SE Coef	T	P
Constant	-0.34143	0.03828	-8.92	0.000
n120	-0.00000051	0.00000578	-0.09	0.930
n135	0.00001522	0.00001051	1.45	0.151
n150	0.00006186	0.00001693	3.65	0.000

S = 0.0993824 R-Sq = 24.4% R-Sq(adj) = 21.9%

Analysis of Variance

Source	DF	SS	MS	F	P
Regression	3	0.293346	0.097782	9.90	0.000
Residual Error	92	0.908672	0.009877		
Total	95	1.202018			

Rearranging the equation above back to the Miner's Rule format we get:

$$0.3414 = \frac{n_{120}}{196{,}000} + \frac{n_{135}}{65{,}700} + \frac{n_{150}}{16{,}170} \quad \text{(Eq. F.2)}$$

Note: The value used for N_{245} is 28.8721 cycles. This was obtained using an IPL/Lognormal best fit to the test data from 235°C and 255°C. Once the acceleration factor is determined the estimated N50% (aka mean life) was calculated at 245°C.

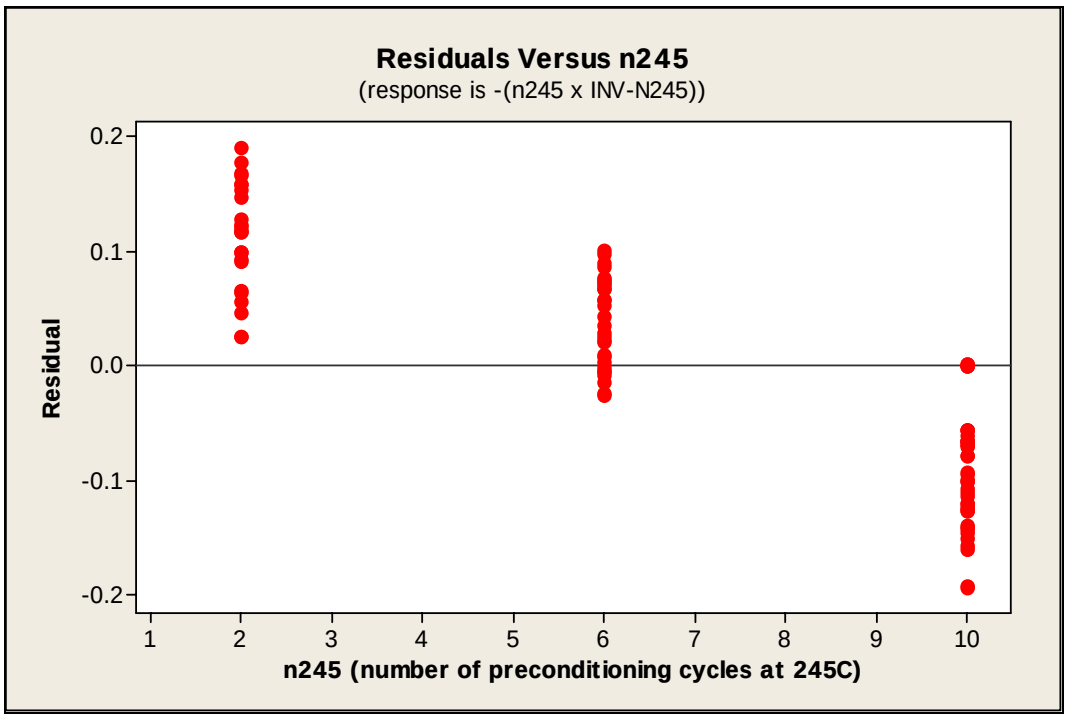

Figure F.3 – Graph shows that the residuals vary with the number of preconditioning cycles at 245°C.

New Methods to Efficiently Test the Reliability of Plated Vias and to Model Plated Via Life from Laminate Material Data

Michael Freda
Sun Microsystems, Inc.
Semiconductor Packaging & PCB Technology

Dr. Donald Barker
University of Maryland
CALCE Electronic Products & Systems Center

IPC Printed Circuits EXPO, APEX and the Designers Summit
22-February-2007

New Methods to Efficiently Test the Reliability of Plated Vias and to Model Plated Via Life from Laminate Material Data

- How thermal stress testing is used at Sun
- Reasons for Sun's PTV reliability work
- Additional results since Sun's last update
- Finite element model
- Model to data correlation
- Summary & conclusions

How Thermal Stress Testing is Used at Sun

- Qualification
  - 3x & 6x thermal stress (IPC-TM-650 2.6.8)
  - APD-Oil-T-Shock (IPC-TR-579)
  - Interconnect stress test (IPC-TM-650 2.6.26)
  - Highly accelerated stress test (MIL-STD-202 Method 107)
  - Kelvin 4-probe of via resistance
    - Measure w/ 4-probe, 6x reflow, measure w/ 4-probe...
- Process control
  - 3x & 6x thermal stress used for routine lot acceptance
  - IST used for product development & quarterly process baseline
  - Sun requires cycling to failure & allows testing at reflow peak

How Thermal Stress Testing is Used at Sun

- Qualification
  - > 3x & 6x thermal stress (IPC-TM-650 2.6.8)
  - > APD-Oil-T-Shock (IPC-TR-579)
  - > Interconnect stress test (IPC-TM-650 2.6.26)
  - > Highly accelerated stress test (MIL-STD-202 Method 107)
  - > Kelvin 4-probe of via resistance
    - Measure w/ 4-probe, 6x reflow, measure w/ 4-probe...
- Process control
  - > 3x & 6x thermal stress used for routine lot acceptance
  - > IST used for product development & quarterly process baseline
  - > Sun requires cycling to failure & allows testing at reflow peak

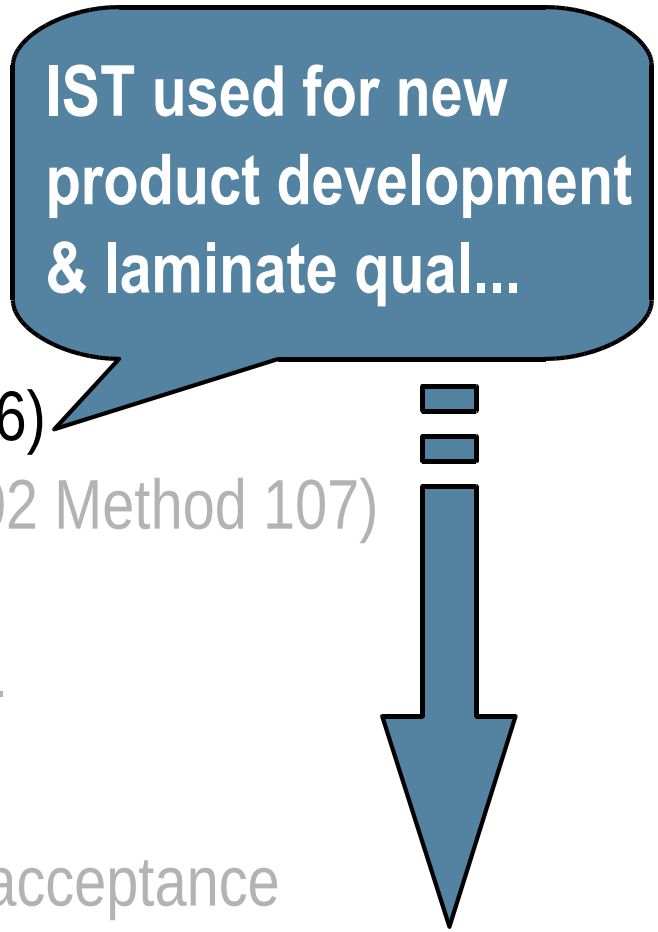

New Methods to Efficiently Test the Reliability of Plated Vias and to Model Plated Via Life from Laminate Material Data

- How thermal stress testing is used at Sun
- Reasons for Sun's PTV reliability work
- Additional results since Sun's last update
- Finite element model
- Model to data correlation
- Summary & conclusions

Reasons for Sun's PTV Reliability Work

- Produce reliable products
  - > “Reliability is the ability to function as expected under the expected operating conditions for an expected time period without exceeding expected failure levels.”
    - Werner Engelmaier
- A need to understand life in the field
- Minimize total cost (laminate test cost, laminate cost, assembly yield, field failures...)
- Shift to lead-free assembly
- Shift to high layer count, aspect ratio >15:1

New Methods to Efficiently Test the Reliability of Plated Vias and to Model Plated Via Life from Laminate Material Data

- How thermal stress testing is used at Sun
- Reasons for Sun's PTV work
- Additional results since Sun's last update
- Finite element model
- Model to data correlation
- Summary & conclusions

Additional Results Since Last Update

- Completed additional IST testing
  - > Increased sample size per test condition
    - One cell at 120°C has only 6 samples
    - All other 13 cells range from 12-24 samples/cell
    - A total of 234 IST coupons cycled to failure
  - > Added test data in the Tg transition zone
    - Test temp include 120°C, 135°C, 150°C, **180°C**, 215°C, 235°C, 255°C, and 275°C

Additional Results Since Last Update, cont'

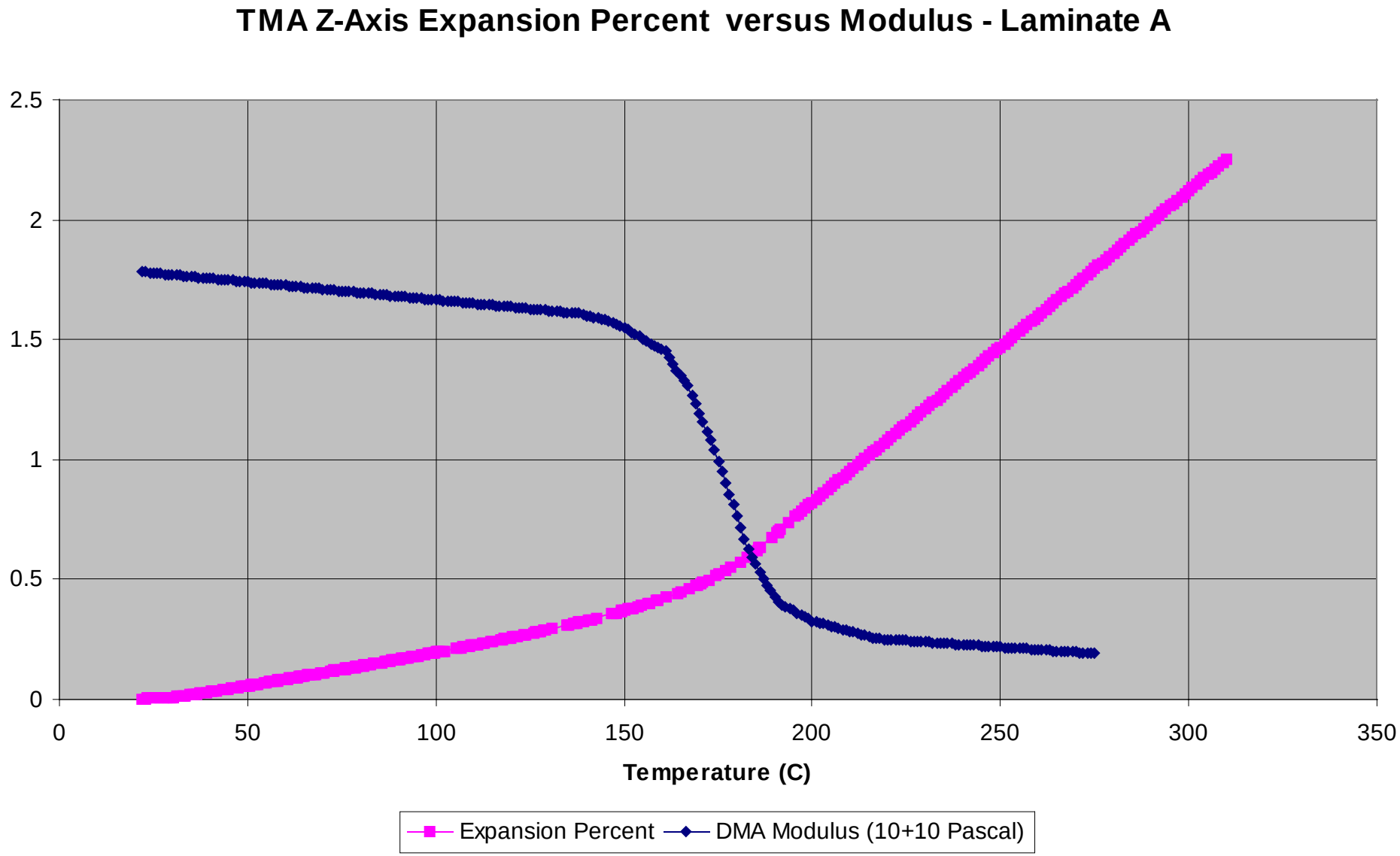

Additional Results Since Last Update, cont'

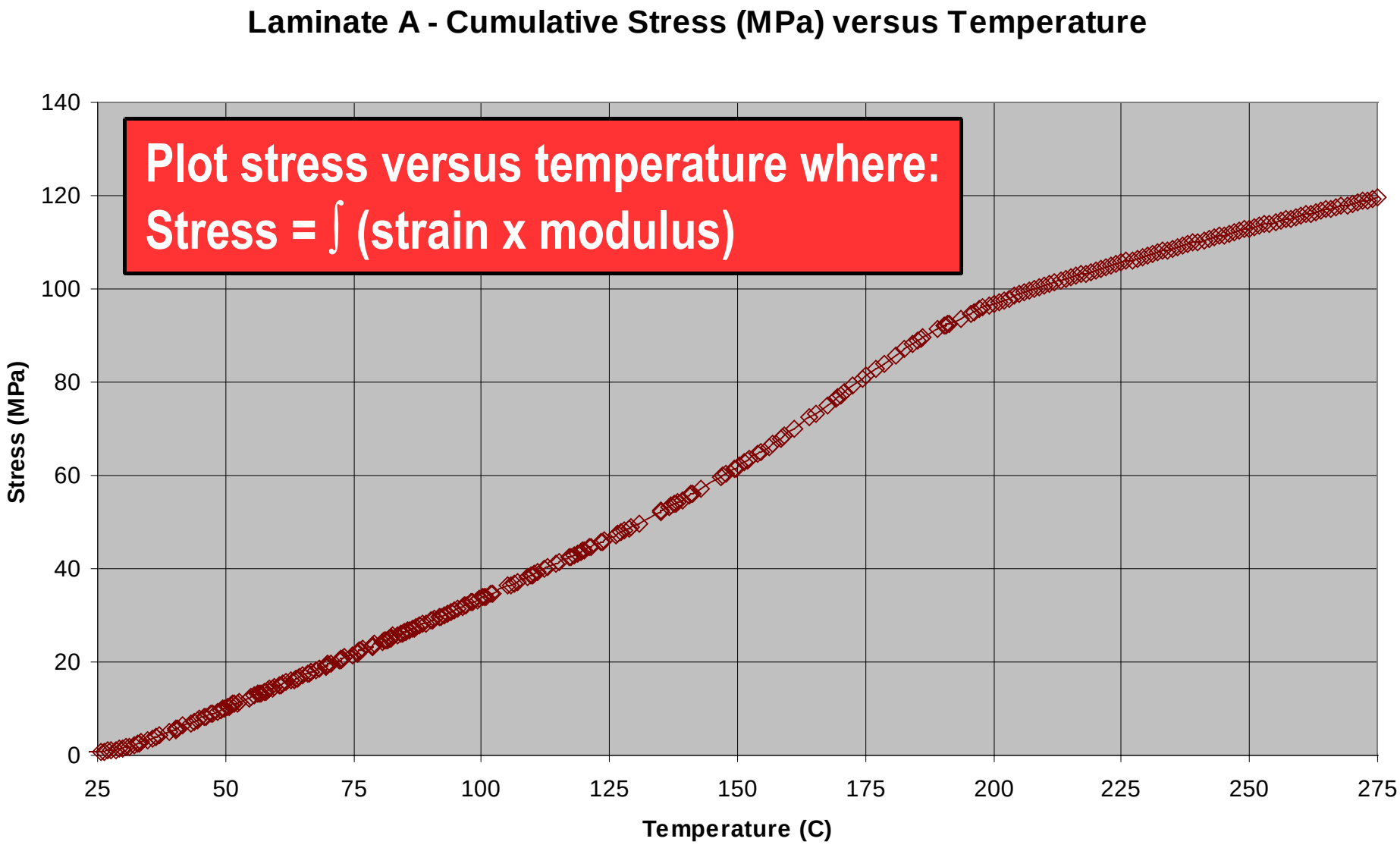

Additional Results Since Last Update, cont'

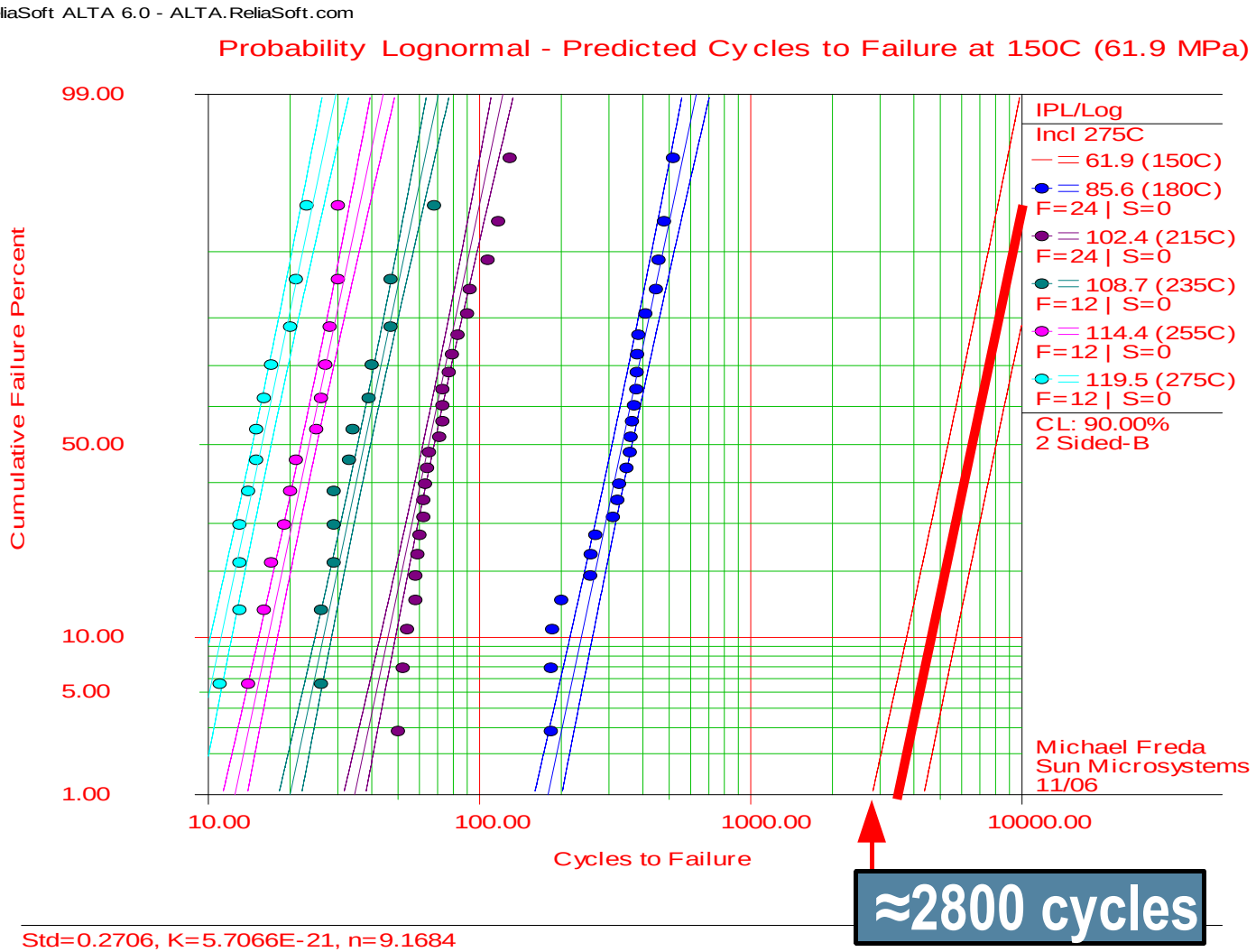

Additional Results Since Last Update, cont'

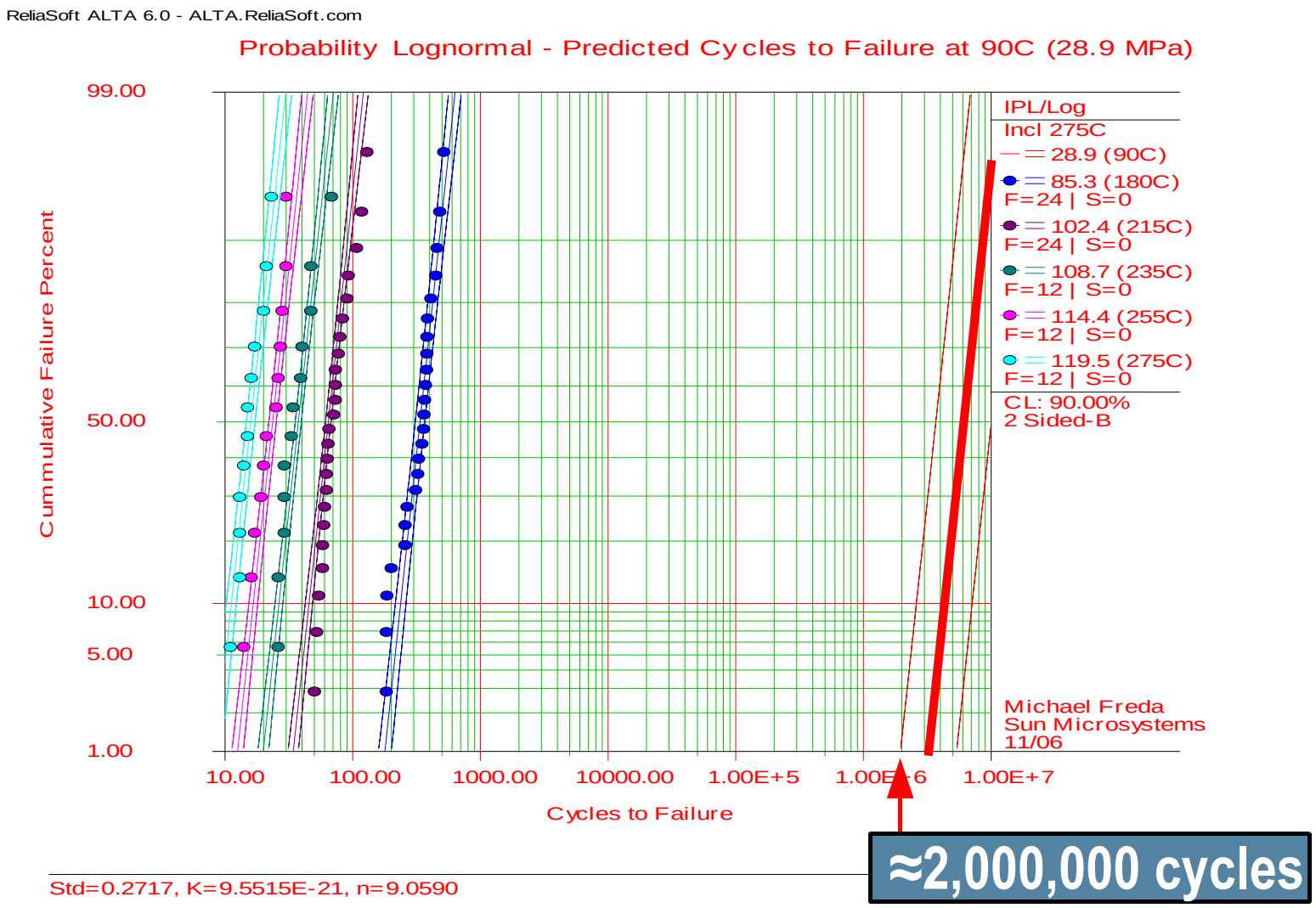

New Methods to Efficiently Test the Reliability of Plated Vias and to Model Plated Via Life from Laminate Material Data

- How thermal stress testing is used at Sun
- Reasons for Sun's PTV reliability work
- Additional results since Sun's last update
- Finite element model
- Model to data correlation
- Summary & conclusions

Finite Element Model - Why?

- Copper properties easy to obtain & they follow the Inverse Power Law (IPL)
  - > Can use Log-Stress to predict Log-N
    - Where N = number of cycles to failure, aka CTF
- Have developed method to understand stress versus temperature for the laminate using TMA & DMA data
- Stress versus temperature using only laminate data is an overly simple 1st order model
  - > We need a more rigourous treatment, finite element analysis
- FEA allows one to compare expected CTF based on laminate material properties
  - > Assumes copper properties & fabrication process constant

Finite Element Model

- The copper in the FEM was modeled as a temperature independent ductile elastic-plastic material following a Ramberg-Osgood constitutive equation:

$$\epsilon = \sigma/E + (\sigma/K)^{1/n}$$

where: **σ = von Mises stress**

ϵ = effective strain (von Mises strain)

E = elastic modulus (120 Gpa)

K = 0.631 Gpa

n = 0.15

Cu CTE = 17 ppm/°C

Poisson's Ratio = 0.35

Finite Element Model – Material Data

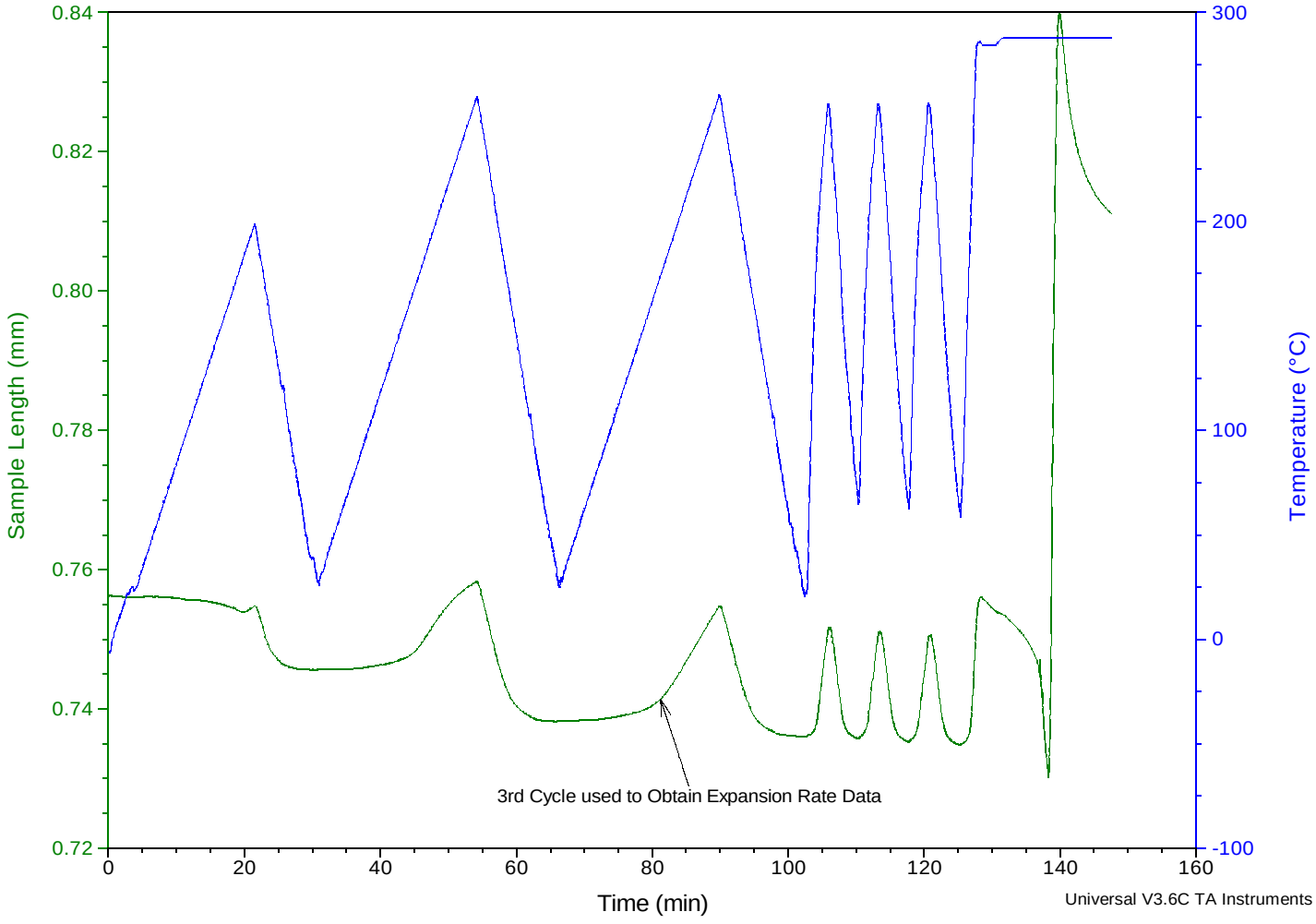

Finite Element Model – Material Data

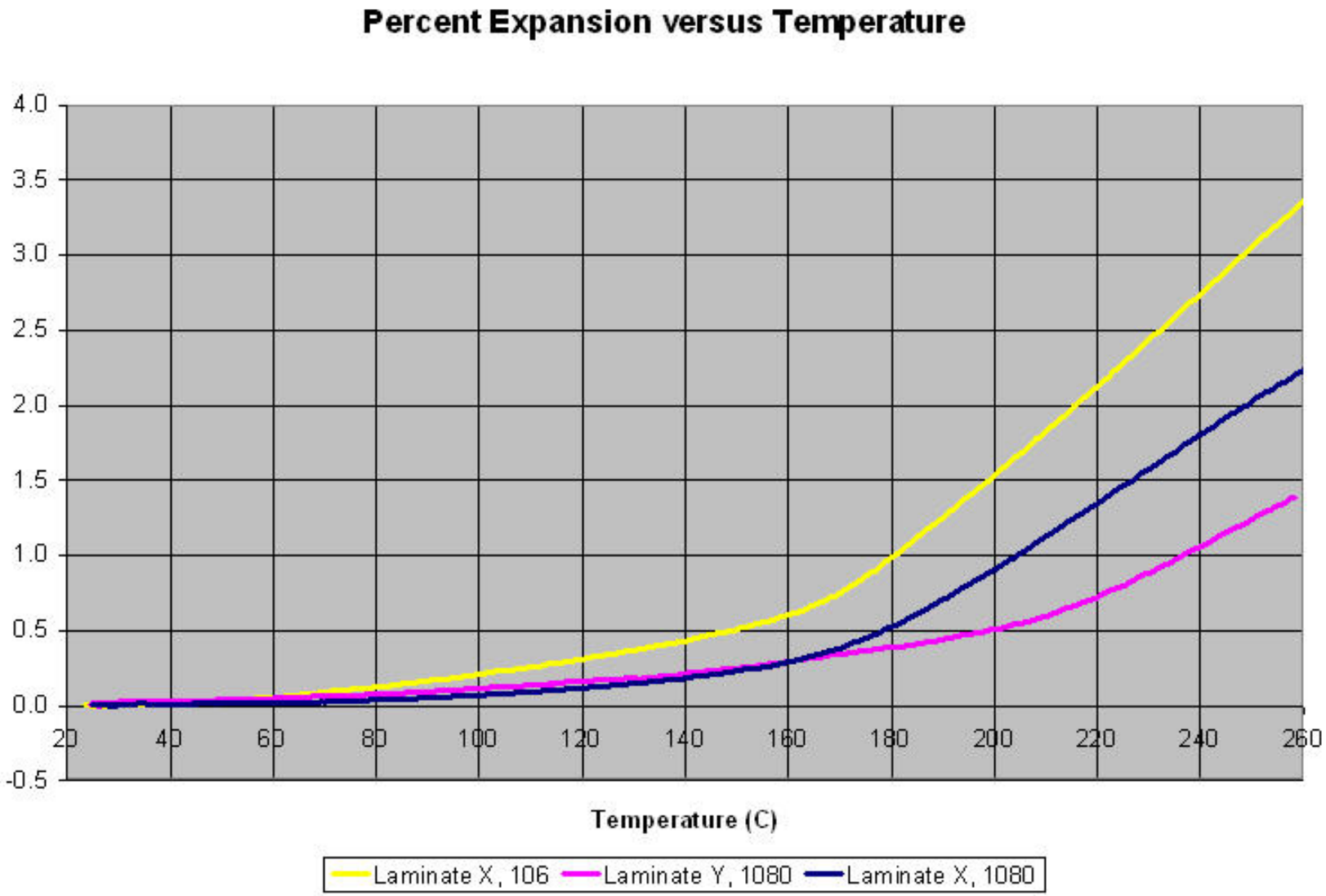

Finite Element Model – Material Data

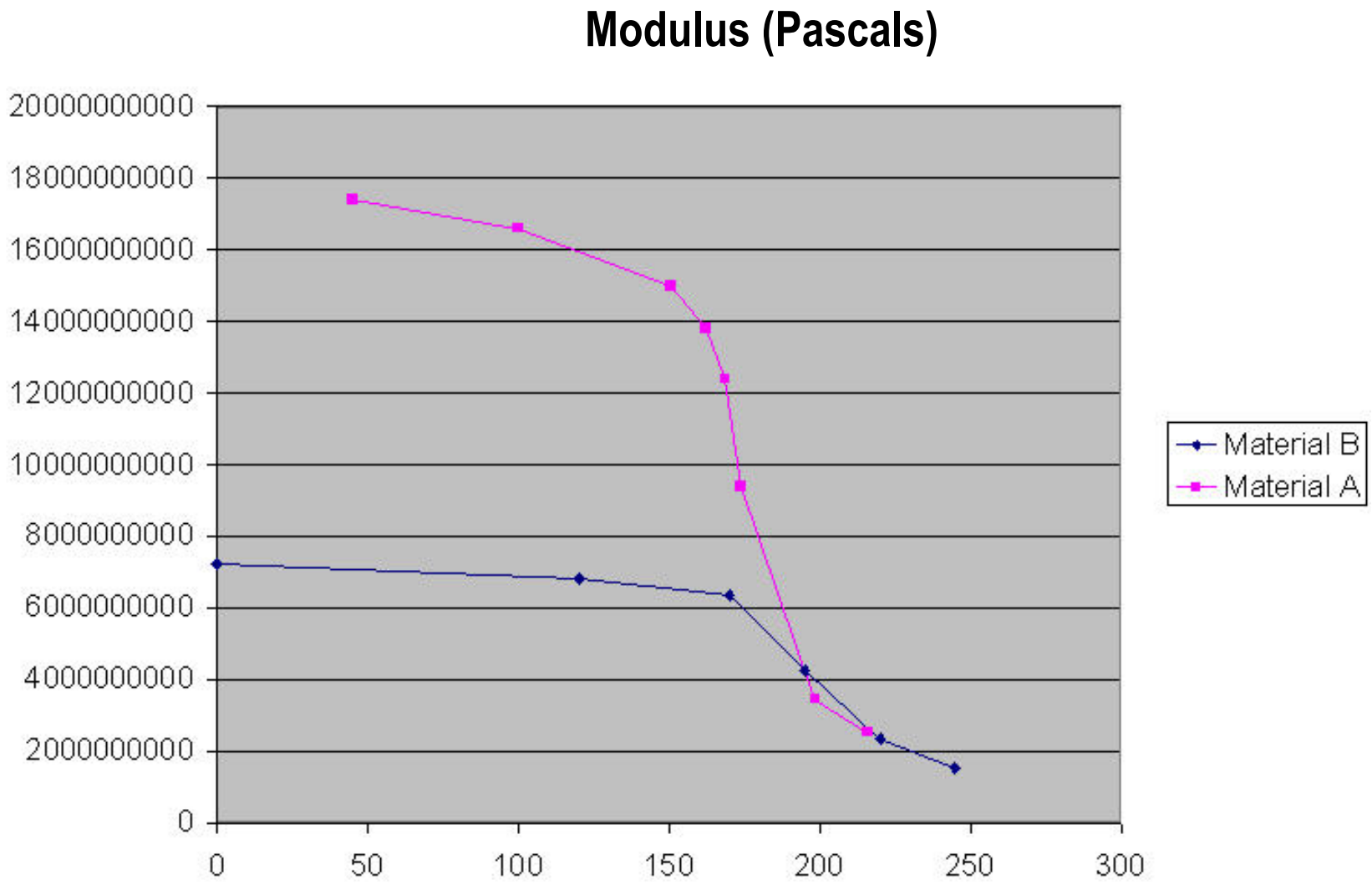

Finite Element Model – Material Data

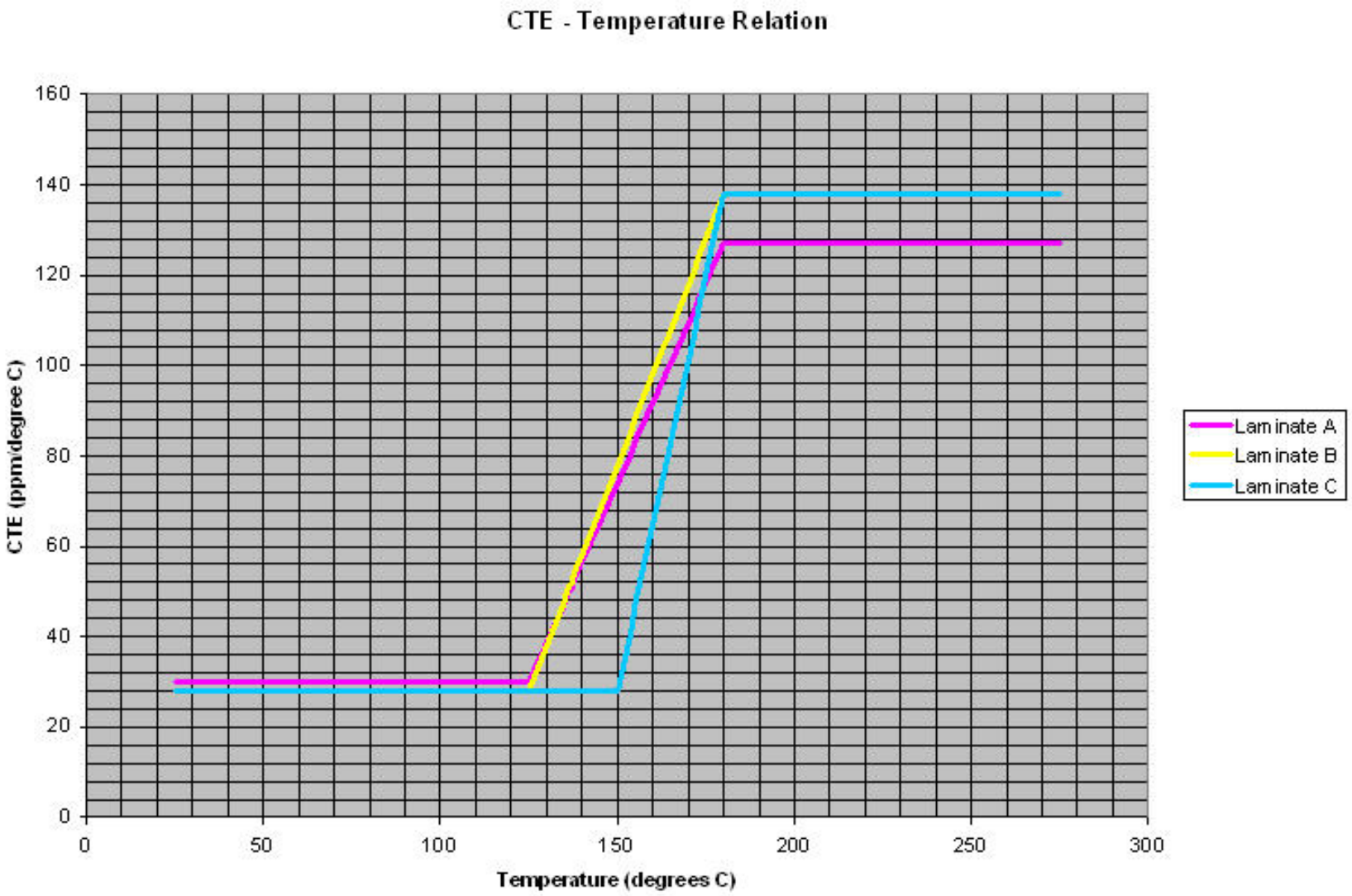

Finite Element Model – Plastic Strain

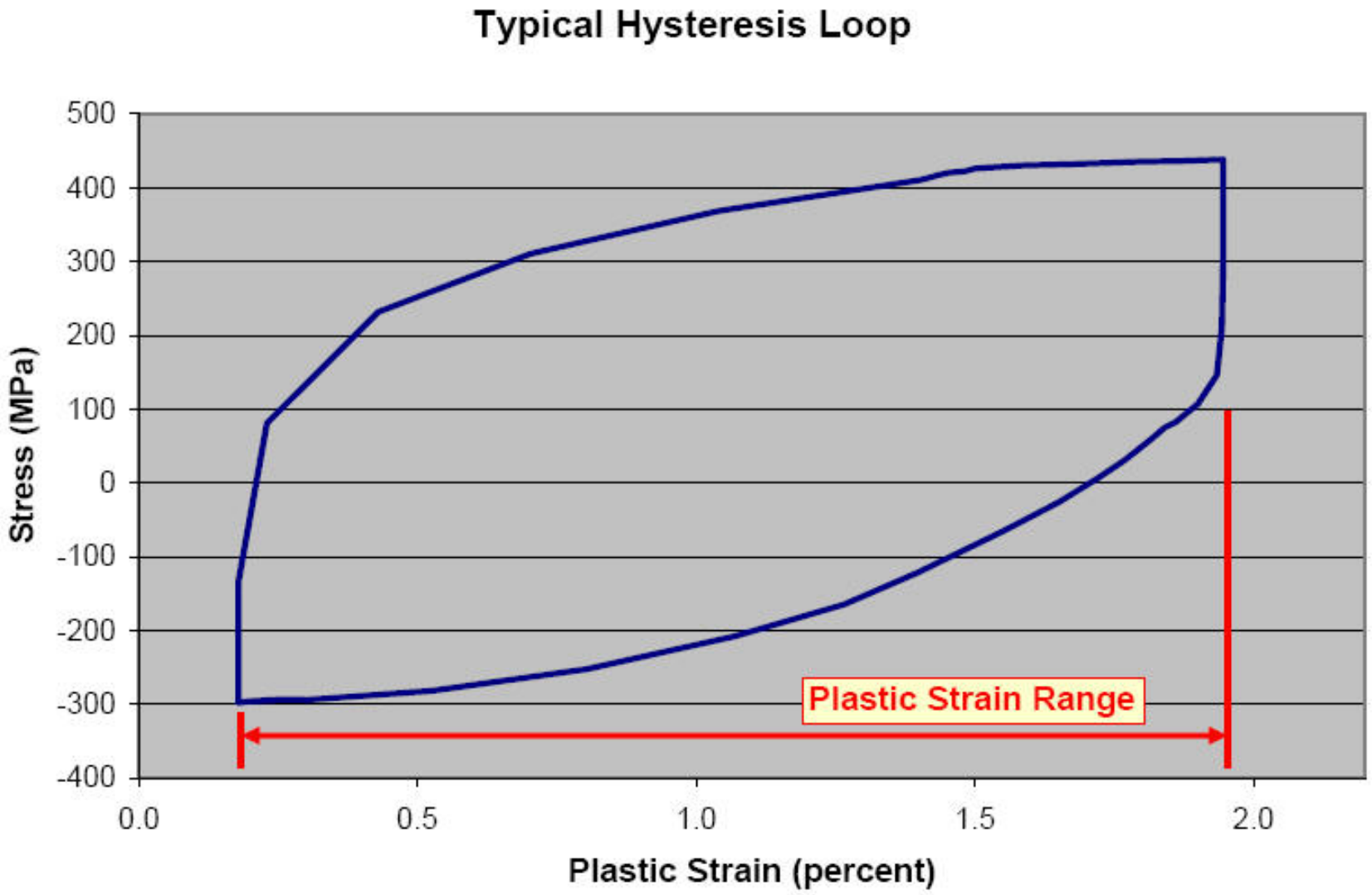

Typical hysteresis loop for the 3rd thermal cycle showing the plastic strain range in the PTH copper barrel.

Finite Element Model – Plastic Strain

- Copper barrel maximum strain range during a thermal cycle, 3mm thick, laminate A

Max Temp - C	Plastic Strain Range (%)	Total Strain Range (%)	Total-Plastic Strain (%)
275	2.554	2.739	0.185
255	2.296	2.505	0.209
245	2.193	2.399	0.206
235	2.091	2.304	0.213
215	1.916	2.114	0.198
200	1.819	2.025	0.206
170	1.342	1.54	0.198
150	0.401	0.604	0.203
135	0.043	0.221	0.178
120	0	0.101	0.101

Finite Element Model – Plastic Strain

- Copper barrel maximum strain range during a thermal cycle, 3mm thick, laminate A

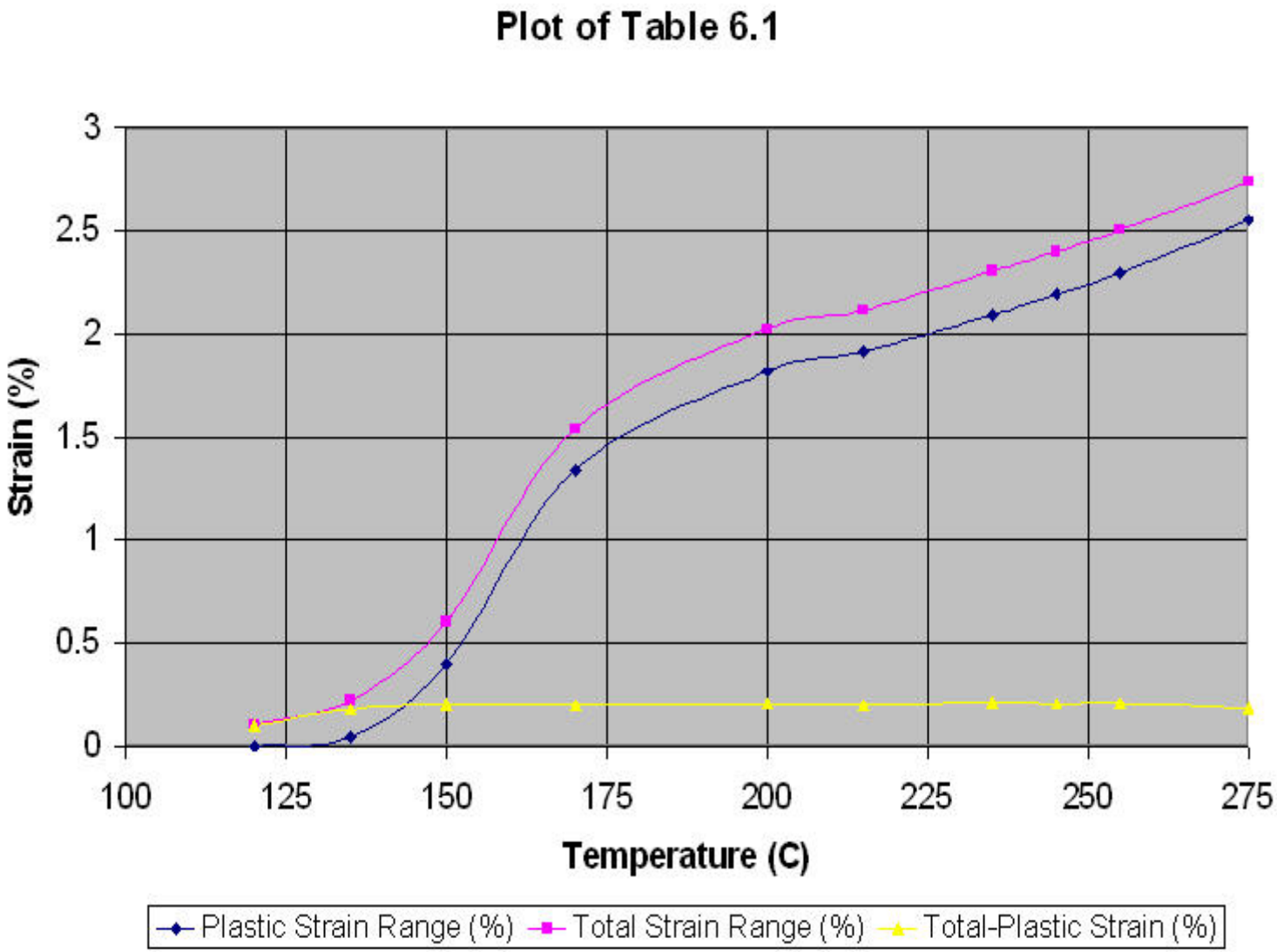

Finite Element Model – Plastic Strain

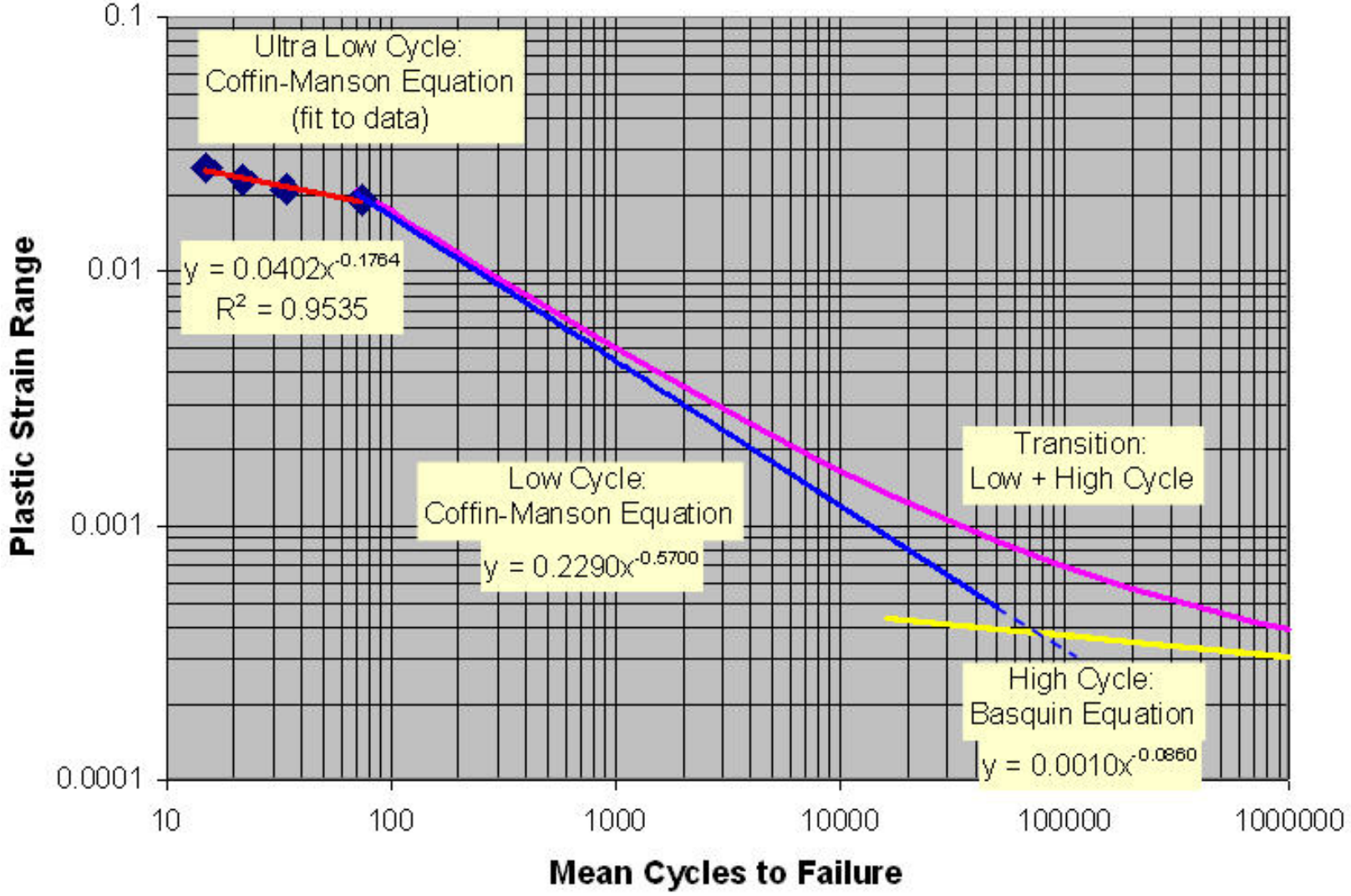

Finite Element Model – Plastic Strain

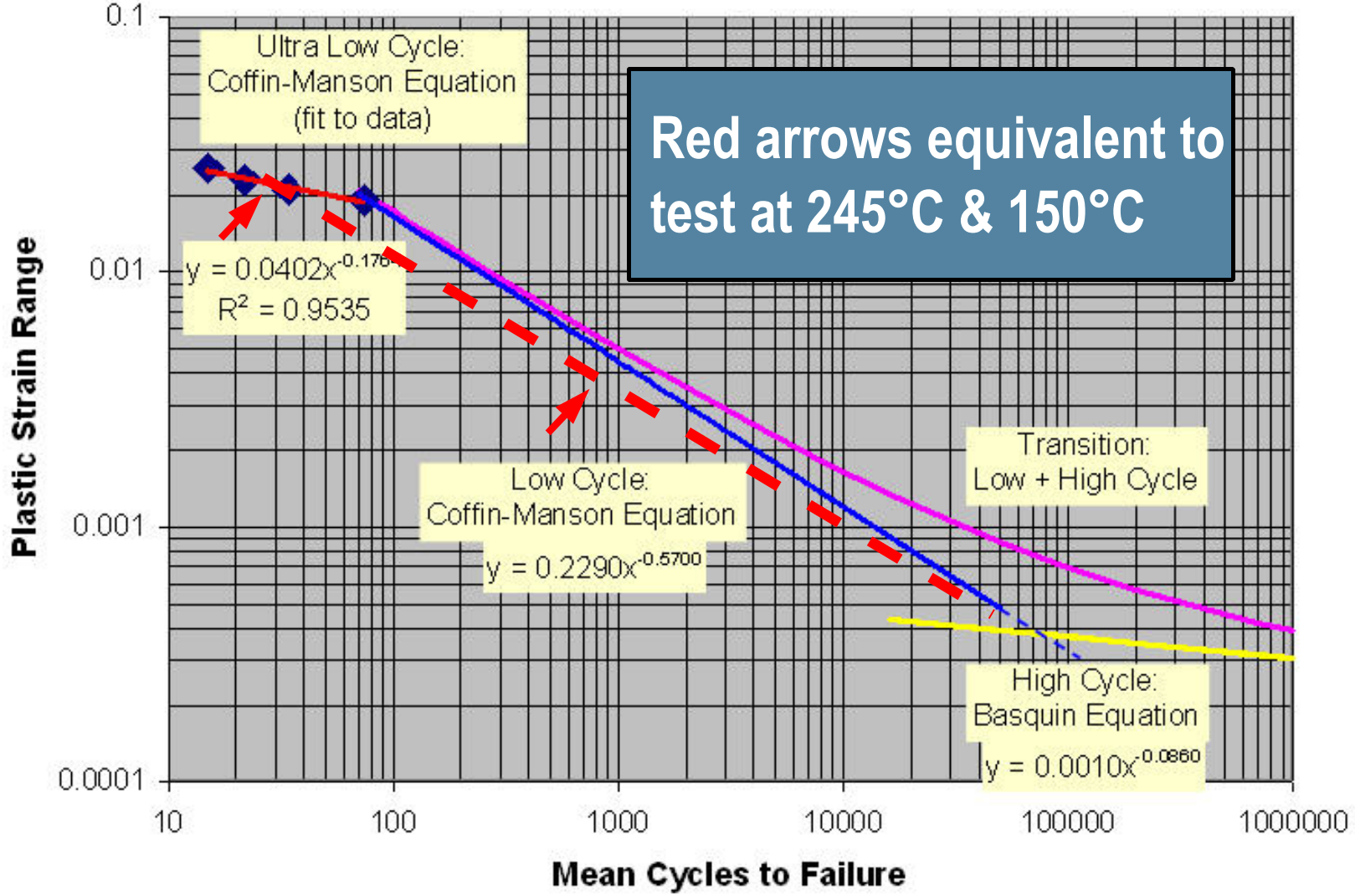

Finite Element Model – Plastic Strain

1. Inverse Power Law: $L(V) = \frac{1}{KV^n}$

2. Manson-Coffin equation: $\frac{\Delta\varepsilon_{plastic}}{2} = \varepsilon_f (2N_f)^c$

3. Manson-Coffin rearranged to IPL format: $N_f = \frac{1}{2}\left[\frac{\Delta\varepsilon_{plastic}}{2\varepsilon_f}\right]^{1/c}$

4. Combined fatigue equation:

$$\frac{\Delta\varepsilon_{total}}{2} = \frac{\Delta\varepsilon_{elastic}}{2} + \frac{\Delta\varepsilon_{plastic}}{2} = \frac{2S_u}{E}(2N_f)^b + \varepsilon_f (2N_f)^c$$

New Methods to Efficiently Test the Reliability of Plated Vias and to Model Plated Via Life from Laminate Material Data

- How thermal stress testing is used at Sun
- Reasons for Sun's PTV reliability work
- Additional results since Sun's last update
- Finite element model
- Model to data correlation
- Summary & conclusions

Model to Data Correlation

- Use cycle to failure estimates from the combined fatigue equation & Miner's Rule to predict field life
  - $$\frac{n_1}{N_1} + \frac{n_2}{N_2} + \cdots + \frac{n_m}{N_m} = C$$
  - $$n_2 = N_2\left(C - \frac{n_{precondition}}{N_{precondition}}\right)$$
    - 2-step process, crack initiation followed by propagation
- Compare model to database from IST testing
- Make predictions of CTF with new laminate

Model to Data Correlation

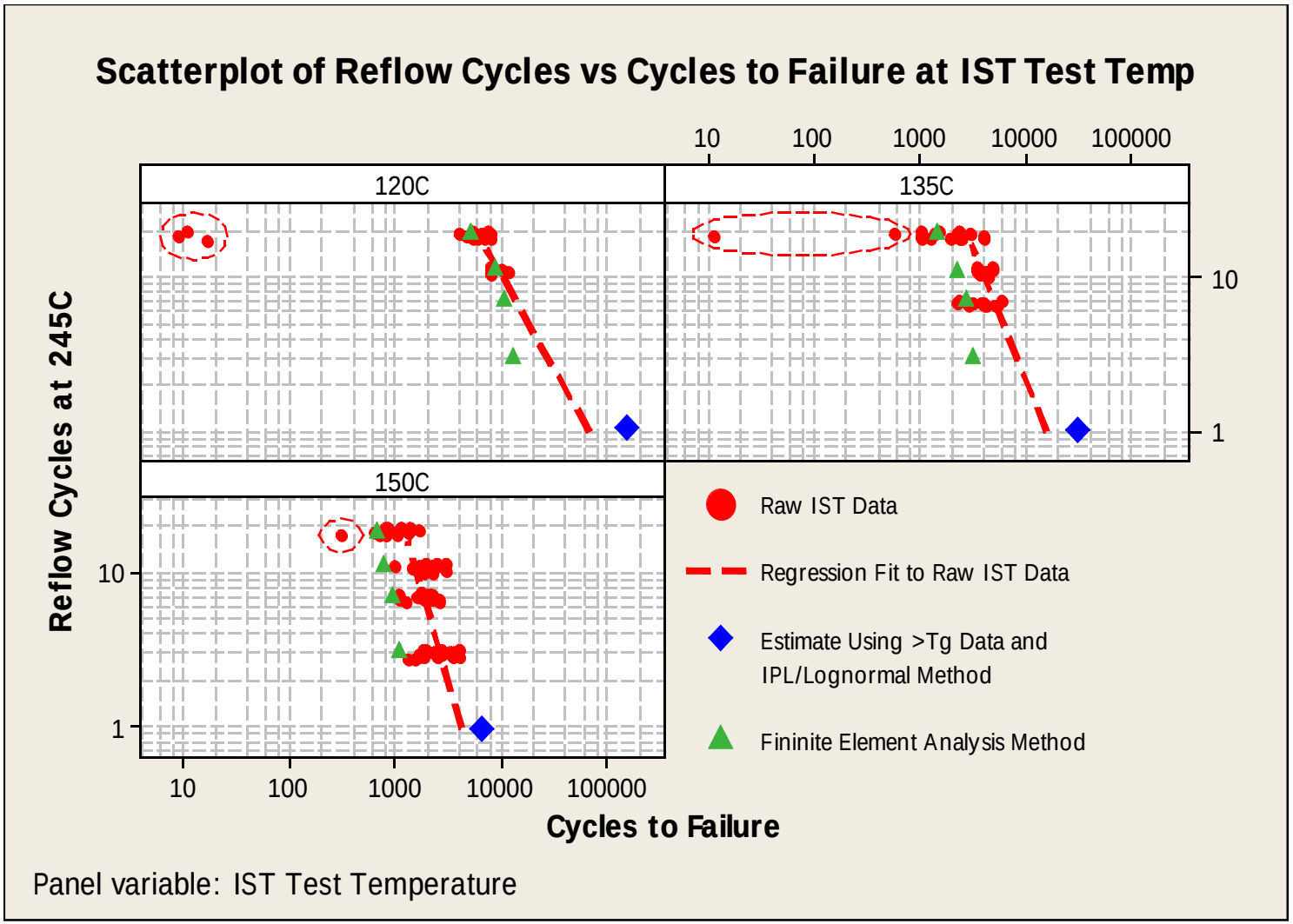

Model to Data Correlation

Using the IPL the ratio of life, N_B/N_A is simply:

$$\frac{N_B}{N_A} = \left(\frac{\Delta\varepsilon_B}{\Delta\varepsilon_A}\right)^{1/c} = (0.86)^{1/-.18} = 2.3$$

Laminate Thickness	Laminate	Plastic Strain Range $\Delta\varepsilon_p$ (%)	Total Strain Range $\Delta\varepsilon$ (%)	$\frac{\Delta\varepsilon_p \text{ B}}{\Delta\varepsilon_p \text{ \_A}}$
3mm	A	2.193	2.399	
	B	1.890	2.103	0.862
6mm	A	2.465	2.673	
	B	2.235	2.433	0.907

Laminate B will last 2.3 times longer than laminate A under a 245°C at 3mm thick

Laminate B will last 1.7 times longer than laminate A under a 245°C at 6mm thick

New Methods to Efficiently Test the Reliability of Plated Vias and to Model Plated Via Life from Laminate Material Data

- How thermal stress testing is used at Sun
- Reasons for Sun's PTV reliability work
- Additional results since Sun's last update
- Finite element model
- Model to data correlation
- Summary & conclusions

Summary & Conclusion

- Have moved from a Log-Stress versus Log-N to a Log-Plastic Strain versus Log-N relationship
  - > More accurate model
  - > Incorporates the non-linear properties of laminate materials
  - > Allows estimates of PTH life from laminate data
    - Assumes fabricator & design are constant
- Able to make a good approximation of CTF with data from testing at two temperatures
- Clearly quantifies laminates that are thermally robust
- Insight into PTH sensitivity to laminate properties

Thank You!
Questions?

Michael Freda
Sun Microsystems, Inc.
Semiconductor Packaging & PCB Technology
Michael.Freda@Sun.COM

Dr. Donald Barker
University of Maryland
CALCE Electronic Products & Systems Center
dbarker@eng.umd.edu

22-February-2007